The Plant Cell, Vol. 22: 2999–3019, September 2010, www.plantcell.org

Structural Sterols Are Involved in Both the Initiation and Tip Growth of Root Hairs in *Arabidopsis thaliana* [W]

Miroslav Ovečka,[a,b,1] Tobias Berson,[c] Martina Beck,[c] Jan Derksen,[d] Jozef Šamaj,[e] František Baluška,[b,c] and Irene K. Lichtscheidl[a]

[a] Core Facility of Cell Imaging and Ultrastructure Research, University of Vienna, A-1090 Vienna, Austria
[b] Institute of Botany, Slovak Academy of Sciences, SK-845 23 Bratislava, Slovak Republic
[c] Institute of Cellular and Molecular Botany, University of Bonn, D-53115 Bonn, Germany
[d] Department of Plant Cell Biology, Radboud University, 6525 ED Nijmegen, The Netherlands
[e] Centre of the Region Haná for Biotechnological and Agricultural Research, Department of Cell Biology, Faculty of Science, Palacký University, CZ-783 71 Olomouc, Czech Republic

Structural sterols are abundant in the plasma membrane of root apex cells in *Arabidopsis thaliana*. They specifically accumulate in trichoblasts during the prebulging and bulge stages and show a polar accumulation in the tip during root hair elongation but are distributed evenly in mature root hairs. Thus, structural sterols may serve as a marker for root hair initiation and growth. In addition, they may predict branching events in mutants with branching root hairs. Structural sterols were detected using the sterol complexing fluorochrome filipin. Application of filipin caused a rapid, concentration-dependent decrease in tip growth. Filipin-complexed sterols accumulated in globular structures that fused to larger FM4-64–positive aggregates in the tip, so-called filipin-induced apical compartments, which were closely associated with the plasma membrane. The plasma membrane appeared malformed and the cytoarchitecture of the tip zone was affected. Trans-Golgi network/early endosomal compartments containing molecular markers, such as small Rab GTPase RabA1d and SNARE Wave line 13 (VTI12), locally accumulated in these filipin-induced apical compartments, while late endosomes, endoplasmic reticulum, mitochondria, plastids, and cytosol were excluded from them. These data suggest that the local distribution and apical accumulation of structural sterols may regulate vesicular trafficking and plasma membrane properties during both initiation and tip growth of root hairs in *Arabidopsis*.

INTRODUCTION

Root hair formation represents one of the best model systems for studying fundamental questions on plant cell polarity, as the axially elongating trichoblasts (root hair–forming epidermal cells) establish a new polarity axis prior to root hair formation. In *Arabidopsis thaliana*, a bulge emerges at a specific site of the outer tangential cell wall of the trichoblast when trichoblast cell elongation is finishing (Dolan et al., 1994; Le et al., 2001). Eventually, this bulge extends laterally and forms a long, tubular root hair. The cytoplasm of an emerging root hair has a distinct polar organization (Bibikova et al., 1997) that is established already during the first steps of bulge formation (Baluška et al., 2000; Grierson and Schiefelbein, 2002). Bulge formation is brought about solely by local cell wall loosening. The cell wall is loosened by a local reduction in the cell wall pH (Bibikova et al., 1998), an increase in the activity of xyloglucan endotransglycosylase (Vissenberg et al., 2001), and the specific expression of expansins 7 and 10 in the trichoblasts (Cho and Cosgrove, 2002). The actin-based tip growth apparatus is established in the outgrowing bulge (Baluška et al., 2000). Cell wall loosening has been reported to be associated with extensive endocytic internalization of degraded cell wall material (Čiamporová et al., 2003). This type of endocytosis resembles the phagocytic internalization of whole *Rhizobia* or so-called infection thread wall degradation vesicles into nodule cells of some legume mutants (reviewed in Baluška et al., 2006). In *Arabidopsis* mutants with weakened cell walls, such as *rsw10* (Howles et al., 2006), *reb1/rhd1* (Andème-Onzighi et al., 2002), and *prc1* (Singh et al., 2008), the whole outer trichoblast cell wall bulges out.

After the actin-based tip growth apparatus is assembled in trichoblasts (Baluška et al., 2000), it starts to drive tip growth (Voigt et al., 2005a). Root hair tip growth depends on signaling molecules, such as stress-induced mitogen-activated protein kinase (Šamaj et al., 2002), as well as on the post-Golgi and endocytotic vesicular trafficking pathways (Ovečka et al., 2005; Šamaj et al., 2005, 2006). These pathways also deliver and recycle some specific cell wall components at the tips of growing root hairs and pollen tubes, such as arabinogalactan proteins and pectins (Šamaj et al., 1999; Lee et al., 2008).

Structural sterols are essential components of the plasma membrane. They are isoprenoid-derived molecules, present as

[1] Address correspondence to miroslav.ovecka@savba.sk.
The author responsible for distribution of material integral to the findings presented in this article in accordance with the policy described in the Instructions for Authors (www.plantcell.org) is: Jozef Šamaj (jozef.samaj@upol.cz).
[W] Online version contains Web-only data.
www.plantcell.org/cgi/doi/10.1105/tpc.109.069880

free sterols and/or in conjugated forms as steryl esters and steryl glucosides in higher plants (Benveniste, 2005). Free sterols carrying a free 3-β-hydroxyl group, such as sitosterol, stigmasterol, and 24-methylcholesterol, are critical for the functioning of membranes (Hartmann, 2004). Cholesterol is a minor component in plants, and it is present only in certain tissues during discrete developmental stages (Hobbs et al., 1996; Arnqvist et al., 2003). In general, the production rate of sterols varies in different cell types. Thus, it is high in proliferating and actively growing tissues, while it declines in mature tissues (Hartmann, 2004). All steps of the biosynthetic pathway of free phytosterols (Benveniste, 1986) as well as the genes responsible for the production of catalyzing enzymes (Bach and Benveniste, 1997) have been described.

Sterols do not only contribute to the structure of the membranes, but they also influence their physical and physiological properties. Sterols interact with proteins and phospholipid acyl chains of the membrane and thus may restrict their motility. In phospholipid bilayers, sterols modify the fluid-like microviscosity and reduce the permeability to small molecules (Mukherjee and Maxfield, 2000). Membrane properties such as composition, width, and (a)symmetry can be changed by certain sterol types (Marsan et al., 1996, 1998). In model membranes, the ratio and chemical structure of sterols determine phase separation, positive or negative curvature, and even vesicle pinching off from the sterol-rich phase (Bacia et al., 2005). Phospholipids interact with sterols via van der Waals and hydrophobic forces (Bessoule and Moreau, 2004). The most important form of interaction, however, occurs by the formation of macromolecular microdomains in the extracellular leaflet, the so-called lipid rafts (Simons and Toomre, 2000), that to a large extent determine membrane specificity, signal perception and transduction, selection of exo-endocytic cargo molecules, as well as intracellular trafficking of sterols (Menon, 2002). The asymmetric distribution of sterol-rich microdomains based on their enhanced detergent resistance and enrichment in glycosylphosphatidylinositol-anchored proteins has been documented also for plant cells (Takos et al., 1997; Peskan et al., 2000).

Genetic studies of the sterol biosynthetic pathway in plants have shown that sterols may regulate and modulate various aspects of plant development (Clouse, 2002). For instance, *STEROL METHYL TRANSFERASE* (*SMT*), a multiallelic gene with several known mutations, is responsible for correct bulk sterol biosynthesis in *Arabidopsis*. Mutation of *SMT1* altered sterol composition, with an enhanced level of cholesterol and a reduced level of typical phytosterols, reduced polar auxin transport, mislocalized PIN1 proteins, and caused several defects in polarity (Diener et al., 2000; Schrick et al., 2002; Willemsen et al., 2003). Mutation of *SMT2* reduced plant growth and fertility (Scheaffer et al., 2001; Sitbon and Jonsson, 2001). Mutation targetting *STEROL C-14 REDUCTASE* (mutant called *fackel*) affects embryo and plant body organization, leading to the dwarf phenotype (Jang et al., 2000; Schrick et al., 2000), and mutation in *STEROL C-8,7 ISOMERASE* (mutant called *hydra1*) leads to aberrant morphogenesis with nonregulated cell size and shape (Souter et al., 2002). Thus, genetic manipulation of sterol composition revealed pleiotropic defects, indicating that structural sterols are indispensable for normal membrane integrity, cell growth, and plant development.

Filipin, a polyene antibiotic fluorochrome, serves as a vital probe suitable for in vivo localization of structural sterols in the plasma membrane of animal (Nichols et al., 2001), yeast (Wachtler et al., 2003), and plant (Grebe et al., 2003; Boutté et al., 2009; Liu et al., 2009) cells. High concentrations of filipin and/or prolonged exposure to filipin effectively induce cross-linking of sterols, which in turn interferes with sterol distribution and function. Filipin treatment that induces deformations of sterol-containing membranes was used as an effective approach for sterol depletion in yeast (Kato and Wickner, 2001; Wachtler et al., 2003) and mammalian (Rothberg et al., 1990; Schnitzer et al., 1994; Shigematsu et al., 2003) cells. Sterol complex formation by cyclic polyene antibiotics like filipin made membranes permeable to ions and small molecules (Kinsky, 1970). In plants, structural changes of the plasma membrane after sterol complexation with filipin were reported using electron microscopy analysis after chemical fixation (Grebe et al., 2003; Boutté et al., 2009) or by freeze-fracture replicas (Moeller and Mudd, 1982).

Besides the receptor-mediated clathrin-dependent endocytosis, sterol-based endocytosis (Grebe et al., 2003; Ovečka and Lichtscheidl, 2006) may also be expected to play an important role in the polar tip growth of plant cells. The sterol endocytic pathway has been shown to interfere with internalization, trafficking, and polar recycling of PIN2, an auxin efflux facilitator and polarity marker in developing root epidermal cells of *Arabidopsis* (Grebe et al., 2003). Sterol-enriched lipid rafts are essential for cellular polarity and proper function of growth apparatus in tip-growing fungal cells (Proszynski et al., 2006; Fischer et al., 2008; Takeshita et al., 2008) and neuronal axons (Guirland et al., 2004; Ibáñez, 2004; Kamiguchi, 2006; Guirland and Zheng, 2007).

Here, we show that local accumulation of structural sterols represents one of the early polarity markers that determine the bulging site in root hair initiating trichoblasts. In addition, structural sterols are reliable markers for the branching points in several mutants of *Arabidopsis* with multiple root hair tips. The presented data suggest that structural sterols are involved in vesicular recycling and endocytosis and in general also in the tip growth of *Arabidopsis* root hairs. Thus, structural sterols emerge as important players in the polar growth of tip-growing plant cells.

RESULTS

Root Tips of *Arabidopsis* and Filipin-Reactive Sterols

Structural sterols form a complex with filipin that can be detected by its fluorescence (Figure 1; Grebe et al., 2003). In growing roots of *Arabidopsis*, the plasma membrane was stained in all cells, indicating that the membranes were rich in filipin-reactive sterols (see Supplemental Figures 1A and 1B online). Membranes in cells of the meristem, transition zone, elongation zone, and root hair forming zone had a comparable intensity of filipin fluorescence, although, due to the presence of lateral root cap cells, the smaller size of meristem cells, and their relatively large surface, the meristem was stained more brightly (see Supplemental Figures 1A and 1B online). In root hairs, the distribution of filipin-labeled sterols depended on the developmental stage (Figure 1A; see Supplemental Figures 1A and 1B online).

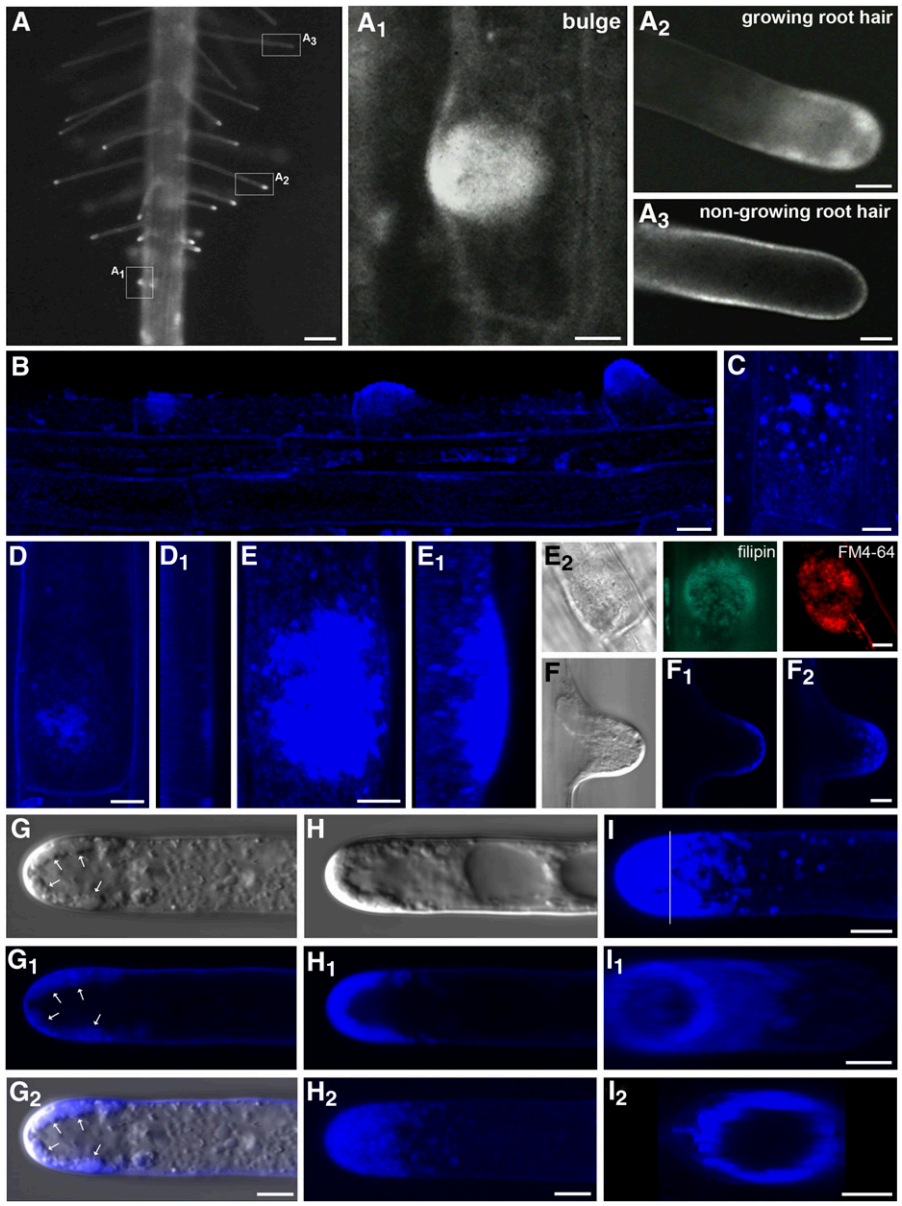

Figure 1. Fluorescence Localization of Sterols in *Arabidopsis* Root by Filipin.

(A) Fluorescence microscopy. Overview of sterol localization in the root hair formation zone. Distribution and accumulation of filipin-reactive sterols reflect the root hair formation process. Zoomed individual stages of bulge formation **(A_1)**, growing root hair **(A_2)**, and nongrowing root hair **(A_3)** shown in boxed areas.

(B) to **(F_2)** Nonuniform distribution of sterols in trichoblasts before and during root hair formation **(B)**. In addition to evenly distributed filipin fluorescence in the plasma membrane, filipin-labeled sterols accumulate in small clusters in the basal pole of trichoblasts before bulge formation (**[B]** to **[D]**, lateral view in **[D_1]**). In the early stages before bulge formation, they are randomly distributed **(C)**. Filipin-reactive sterols are strongly enriched in the bulge (**[E]**, lateral view in **[E_1]**) and in the emerging tip of the root hair (**[F]** to **[F_2]**). Globular filipin-induced structures enriched in the bulge coaccumulate FM4-64 **(E_2)**.

(G) and **(H)** Accumulation of sterols in growing root hairs. Formation of apical sterol-rich clusters (arrows) after prolonged filipin treatment (**[G]** to **[G_2]**). Filipin-sterol complexes are predominantly formed in the apical and subapical zone of the growing root hair (**[H]**, single median section in **[H_1]**, z-projection in **[H_2]**).

(I) Cross section of the basal part of the apex (position marked by line in **[I]**) and rotation revealed that filipin-sterol complexes are closely associated with the plasma membrane (**[I_1]** and **[I_2]**).

(B) to **(I)** Confocal microscopy; **(F)** to **(H)** differential interference contrast (DIC) images; and **(G_2)** confocal-DIC merged image. Bars = 100 μm in **(A)**, 10 μm in **(B)**, and 5 μm in **(A_1)** to **(A_3)** and **(C)** to **(I)**.

Sterols Are Enriched at the Tips of Growing Root Hairs

At root hair formation (see Supplemental Figure 1 online), the distribution of sterol-rich domains correlated with the ongoing developmental program. A polar accumulation of sterols occurred in the short period of trichoblast development. Higher sterol-specific fluorescence signals were found in the prebulge stage, in root hair bulges, and in the tips of growing root hairs (Figure 1; see Supplemental Figures 1A and 1B online).

Filipin-positive sterols accumulated in globular structures located in the trichoblast cell's cortex prior to bulge formation (Figures 1B to $1D_1$; see Supplemental Movie 1 online). Similar globular structures were also present in the bulges (Figures $1A_1$, 1E, and $1E_2$; see Supplemental Movie 2 online) and growing root hair tips (Figures 1F and $1F_2$). The plasma membrane was labeled evenly in the trichoblast cell body and in the flanks of the entire root hair (Figures $1A_2$, $1G_1$, $1H_1$ to $1H_2$, and 1I), but differently sized globular particles with structural sterols accumulated in the tip region (Figures $1A_2$, 1G to $1G_2$, and 1H to H_2). The distribution of these structures correlated with the internal polarity of the cytoplasm, and most of them were found in the very tip and in the subapical region. By contrast, no filipin-positive particles were seen in the cytoplasm of growth-terminating and mature root hairs (Figures 1A and $1A_3$; see Supplemental Figures 1A and 1B online). There, only the plasma membrane was labeled, but it did not show any gradients or any preferred sterol accumulating domains (Figure $1A_3$). Thus, the appearance of filipin-positive compartments in the apical cytoplasm of root hairs completely depends on their polar tip growth activity.

Sterol Redistribution and Local Accumulation Occur before Visible Root Hair Formation

In the very early prebulge stage of trichoblast formation, sterols were distributed evenly over the entire plasma membrane (see Supplemental Figures 1A and 1B online; Grebe et al., 2003). Before the emergence of a bulge, however, a striking change in fluorescence distribution occurred. In this early stage of bulge formation, filipin-positive patches were observed at the basal pole of the trichoblasts (Figures 1B and 1C; see Supplemental Figure 2 online). Subsequently, an intensive circular sterol-positive disc arose in the basal end (closer to the root apex) of the trichoblast where the bulge and future root hair would later appear, at the so-called prebulging site (Figures 1B to $1D_1$; see Supplemental Movie 1 online). Remarkably, the first increase of polar fluorescence appeared before structural signs of bulge formation became visible. Intensive fluorescence remained when the prospective bulge emerged as a morphologically visible structure protruding out of the trichoblast. The distribution of filipin-reactive sterols, which accumulated selectively in the emerging tips, reflected the internal architecture of the bulge (Figures 1A, $1A_1$, and 1E to $1E_1$). The intensive fluorescence did not originate from the plasma membrane alone, but mainly from small filipin-positive particles that accumulated abundantly below the plasma membrane of a selected domain in the cortical cytoplasm, within the future site of bulge formation or at the bulge itself (Figures $1D_1$ and $1E_1$; see Supplemental Movies 1 and 2 and Supplemental Figure 2B online). These particles are most likely derived from the plasma membrane by endocytosis because filipin can bind only to the outer leaflet of the plasma membrane (Grebe et al., 2003). This is further supported by specific staining of bulges with FM4-64 (Figure $1E_2$).

A close association of filipin-positive compartments with the tip was evident not only in trichoblasts but also in growing root hairs. Filipin-sterol complexes were predominantly formed in the apical zone of growing root hairs (Figures 1G to H_2). Staining of the plasma membrane of root hairs by filipin was evident in flank regions (Figures $1A_2$, $1G_1$, $1H_1$, $1H_2$, and 1I). Clear plasma membrane (but not cell wall) staining occurred also in the tip of root hairs after plasmolysis (see Supplemental Figure 3 online). In addition, fluorescence intensity profiles from optical cross sections of the basal part of the root hair apex showed that filipin-sterol complexes were closely associated with the plasma membrane from the inner side (Figures 1I to $1I_2$). Thus, we conclude that compartments derived from the plasma membrane that physically interact with the plasma membrane and adjoin internalized endocytic vesicles were stained by filipin as well.

Sterols as Reliable Markers of Branching Points in Multiple Root Hairs

Branching of root hairs in the *tip1* mutant starts already at the bulge stage and leads to the formation of double, triple, or quadruple branches. Before branching, bulges have a widened base (Figure 2A) with edges (Figure 2B) that are able to produce individual growing tips (Figure 2C). In the case of double branching, the growth rate of both tips is comparable, mostly producing two hair tubes of equal size (Figure 2D).

Already in the single bulge, filipin-sterol complexes were partitioned into two distinct domains within the apical part (Figure 2E). This dichotomy was even more pronounced when the bulge's leading edges became clearly established (Figure 2F). Sterol accumulation was strictly tip focused in the two outgrowing hairs (Figure 2G). When even more tips arose from the common bulge, a broad widening of the bulge preceded their radial outgrowth. At this stage, site selection was not specified, future polarity was not yet established, and filipin-sterol complexes decorated the entire plasma membrane (Figure 2H). In double-branched growing root hairs as well as in triple- and multiple-branched hairs, sterols accumulated only in growing tips (Figure 2I). When some of these branches of multiple hairs terminated their tip growth, the localized sterol accumulation disappeared in these branches but remained tip focused in the growing tips (Figure 2J).

Mutation of the *HYDRA2* locus interferes with the root hair phenotype, resulting in deviant shapes, bifurcation, and side branch formation (Souter et al., 2002). Sterol accumulation in the growing tip appeared to be unaffected (Figure 2K), but a few discernable domains were recorded along the surface of the flanks in the root hairs of the *hydra2* mutant (Figures 2K and $2K_1$). Close inspection of these branching root hairs revealed that filipin-labeled domains along the lateral surface were selection points for new tips of the future lateral branch (Figures 2L and $2L_1$). Finally, tips from both primary and branching hairs displayed apical sterol accumulations (Figures 2L and $2L_1$). Thus,

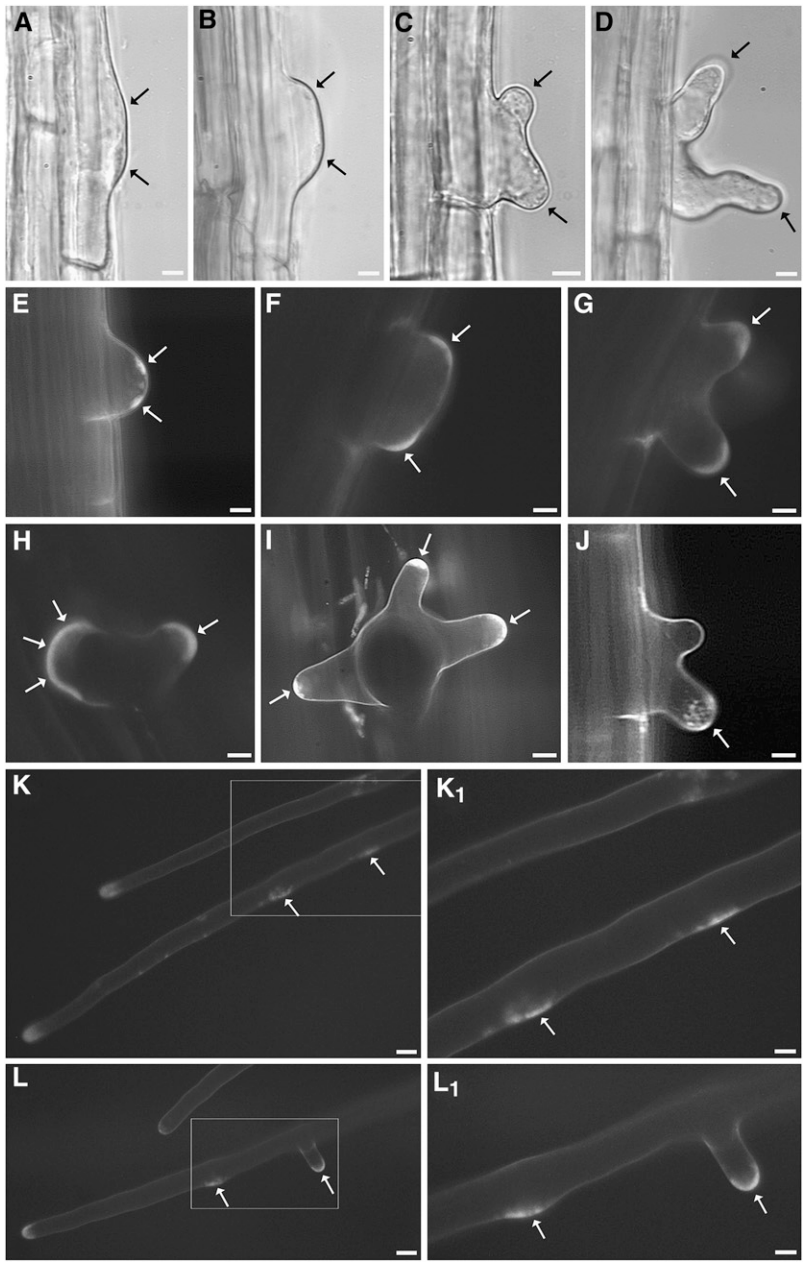

Figure 2. Sterols in Branching Domains of Multiple Root Hairs.

(A) to **(D)** Typical branching phenotype of *tip1* root hair mutant starting in the early stage of bulge formation. From the preformed edges of the common bulge, more than one growing hair tip is produced.

(E) to **(G)** Two future outgrowths from the unitary bulge are predicted by filipin-sterol complexes localized in two distinct domains within the apical part of the bulge.

(H) to **(J)** During the broad widening of the bulge preceding multiple tip formation, filipin-sterol complexes decorated the plasma membrane surrounding the entire broadened region. In multiple root hairs, sterols accumulated in growing tips. In multiple root hairs with growing and nongrowing branches, localized sterol accumulation was a typical feature of only the growing tip but disappeared from the nongrowing one.

(K) Root hair phenotype of the *hydra2* mutant showing the formation of side branches on the root hair tube. Sterols accumulate in the main growing tip of the root hair and in some other localized domains marked by filipin along the side surface of the hair tube (area selected in box is enlarged in **[K_1]**).

(L) From filipin-positive preselected domains, new growing tips arise that express typical tip-focused sterol accumulation during tip growth (area selected in box shown in detail in **[L_1]**).

(A) to **(D)** DIC images and **(E)** to **(L_1)** fluorescence microscopy. Leading edges of growing root hair tips are indicated by arrows. Bars = 10 μm in **(K)** and **(L)** and 5 μm in **(A)** to **(J)**, **(K_1)**, and **(L_1)**.

localized accumulation of sterol-rich membrane domains and their enrichment in the cortical cytoplasm is not only a typical feature of growing root hair tips but most probably also plays an active role in the selection process and in the maintenance of the site of future tip growth.

Dose-Dependent Complexation of Sterols by Filipin Inhibits Root Hair Tip Growth

Intensive sterol labeling with filipin (Figure 1) interfered with the motility of particles in the tip. We therefore addressed the question of whether high concentrations of filipin or prolonged exposure could induce cross-linking of sterols and thus interfere with their function and distribution. We correlated different concentrations of filipin with the growth rate of root hairs using time-lapse video imaging techniques and characterized root hair tip growth, cytoarchitecture, morphology, and intracellular motility in the tip. For that purpose, we had to make sure that root hairs were not affected by mechanical manipulation during the experiments. Transfer of seedlings from the agar plate to the microscope as well as tiny changes of the medium composition rapidly inhibit tip growth. Therefore, root hairs were grown in microscopic chambers that provided a controlled, stable environment and that allowed the monitoring of development and growth thoroughly in each experiment. This allowed us to measure root hair growth constantly while avoiding any external manipulation. Under these conditions, any response of growing root hairs can be considered as an immediate reaction to the altered state of structural sterols affected by filipin.

Application of filipin caused a rapid decrease in tip growth rate in a concentration-dependent manner (Figures 3A and 3B). The growth rate of control root hairs within a 15-min period of observation was 1.76 (± 0.36 SD) $\mu m \cdot min^{-1}$ (Figure 3C). Root hairs grew at similar rates (1.78 [± 0.1 SD] $\mu m \cdot min^{-1}$) in the presence of 0.1 $\mu g \cdot mL^{-1}$ filipin. Their growth slowed down slightly to 1.48 (± 0.1 SD) $\mu m \cdot min^{-1}$ in 1 $\mu g \cdot mL^{-1}$ filipin. However, tip growth was dramatically reduced to 0.38 (± 0.14 SD) $\mu m \cdot min^{-1}$ and 0.22 (± 0.12 SD) $\mu m \cdot min^{-1}$ in 5 and 10 $\mu g \cdot mL^{-1}$ filipin, respectively (Figures 3A, 3B, and 3D). Inhibition started very rapidly, already at the time of perfusion (Figure 3B). A strong reduction in growth correlated with those concentrations of filipin that yielded strong fluorescence, suggesting that sterol detection in the tip (Figure 1) was accompanied by the formation of large filipin-sterol complexes. These experiments show that sterols are important factors in the progression of root hair tip growth. When the sterol trafficking and function are compromised by complexation with filipin, tip growth is affected considerably.

Complexation of Sterols Affects the Cytoarchitecture at the Tip of Growing Root Hairs

Analysis of root hair growth rate using video recording at high magnification generated valuable data about the shape of the apex, length of the clear zone, and the motility and directional movement of vesicles and globular particles. A reduction of growth correlated with severe changes of the cytoarchitecture in the tip. Both control (Figure 3C) and filipin-treated (0.1 and 1 $\mu g \cdot mL^{-1}$) root hairs displayed the typical polar organization. The clear zone within the dome-shaped tip was filled with small vesicles. The clear zone was followed by a region that exhibited streaming. Larger organelles, including the nucleus and vacuole, were excluded form the tip and cytoplasmic streaming followed the classic type of reverse fountain-like streaming (see Supplemental Movie 3 online).

After treatment with 10 $\mu g \cdot mL^{-1}$ filipin, tip growth of root hairs stopped almost completely (Figures 3A, 3B, and 3D) and the root hairs exhibited dramatic changes in morphology; motility and tip-directed movement of vesicles were blocked and the very tip was occupied by enlarged dense aggregates. Most of the aggregates were closely associated with the apical plasma membrane (Figure 3D; see Supplemental Figure 4 and Supplemental Movie 4 online). Sterols within the trapped aggregates at the tip were always strongly labeled by filipin (Figures $1A_2$ and 1G to $1H_2$). This indicates a correlation with severe changes in the cytoarchitecture of the tip and a massive reduction of tip growth after modification of available sterols.

Complexation of Sterols Affects the Motility of Vesicles at the Tip of Growing Root Hairs

Vesicles in the tip of growing root hairs are too small to be discerned by a conventional light microscope. Therefore the vesicle-rich apical zone was termed the clear zone (Campanoni and Blatt, 2007). In this study, we used video microscopy in combination with contrast enhancement by computer processing to visualize small vesicles in root hairs. We could observe their trajectories, as well as the lengths and directions of their movements. In control conditions, the motility of organelles differed in the apical and subapical zone of the root hair. In the tube, larger and smaller organelles moved fast and were directed along the axis of the tube for nanometer- or micrometer-long distances, interrupted by pauses of irregular length. Although each organelle had its individual pattern of direction and velocity, they together appeared to move in a coordinated fashion (see Supplemental Movie 3 online). This was not the case in the clear zone. The small vesicles here vacillated quickly in an irregular and uncoordinated, but active fashion similar to Brownian motion. Occasionally, particles could embark directly from Brownian to directed movement. However, single vesicles then followed long trajectories that were seldom straight but mostly curved and bent, interrupted by pauses between shorter or longer distances (see Supplemental Figures 4A and 4B and Supplemental Movie 3 online).

Filipin had a considerable effect on the movement of vesicular organelles. In the clear zone, together with rapid reduction of the tip growth rate (Figure 3B), particles slowed down soon after treatment and displayed only a Brownian type of movement. Finally, they became immobilized at the plasma membrane (see Supplemental Figures 4C to 4E and Supplemental Movies 4 and 5 online). After the clear zone was lost, the tip was invaded by reticulated vacuoles. In the subapical region, fast and straight long distance movement disappeared; particles moved for shorter distances and made longer breaks (see Supplemental Movies 4 and 5 online). Organelles in the tube were more protected to maintain their directed movement. However, when

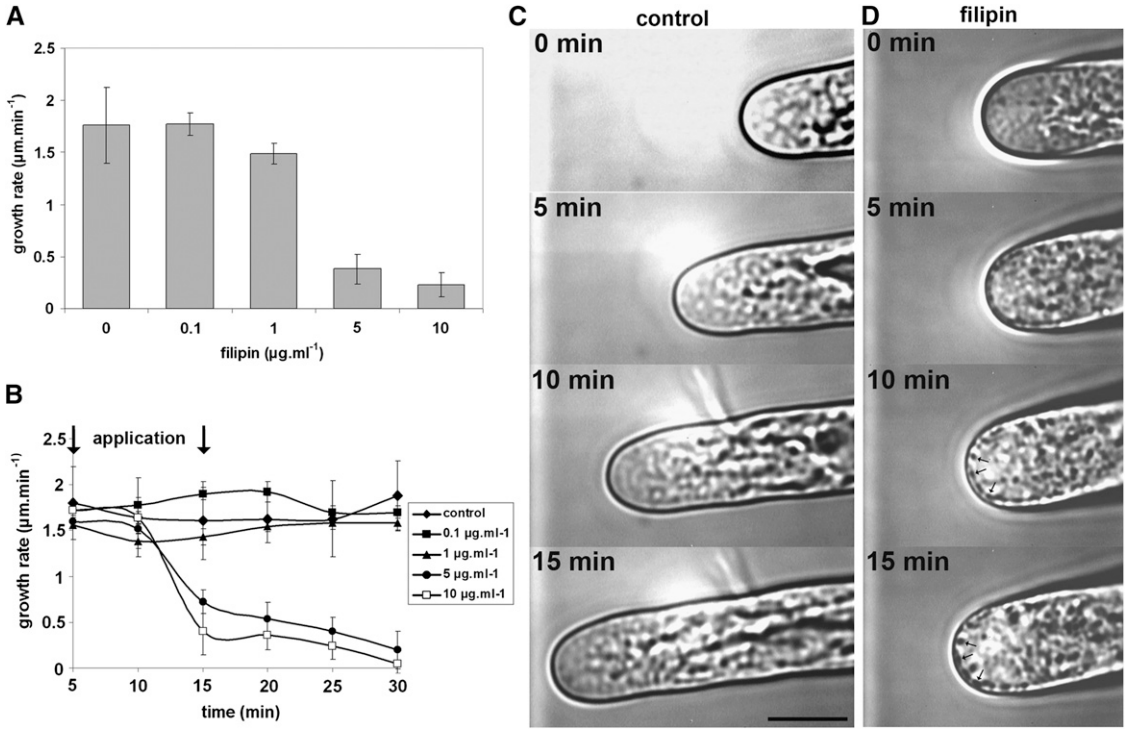

Figure 3. Tip Growth after Complexation of Sterols.

(A) Mean growth rate of root hairs treated with filipin (±SD, the sample sizes are 5 to 19 root hairs). Roots were perfused with different concentrations of filipin for 10 min, and the growth rate of root hairs was recorded for 15 min.

(B) Time-dependent reaction of root hair tip growth to filipin (±SD, the sample sizes are 5 to 19 root hairs). Time period of the application is indicated by arrows. Note the decrease of tip growth immediately after the application of 5 and 10 $\mu g \cdot mL^{-1}$ filipin.

(C) and **(D)** Root hairs perfused with control medium for 10 min (0 min in **[C]**) show a normal rate of tip growth within 15 min, while root hairs perfused with 10 $\mu g \cdot mL^{-1}$ filipin for 10 min (0 min in **[D]**) stopped growth almost completely. In addition to growth reduction, changes in the cytoarchitecture of the clear zone and formation of filipin-induced apical compartments (arrows in **[D]**) have been induced. Bright-field images from video microscopy. Bar = 10 μm.

particles progressed into the modified tip, they soon stopped moving (Figure 3D; see Supplemental Figures 4C to 4E and Supplemental Movies 4 and 5 online). Despite these dramatic changes in vesicle and organelle dynamics in the growing root hairs, organelle movement was unaffected in mature root hairs (see Supplemental Movie 6 online), atrichoblasts (see Supplemental Movie 7 online), and cortex cells (see Supplemental Movie 8 online). Clearly, the high sensitivity of the tip-growing domains in root hairs to agents such as filipin is reflected in a perturbation of the intracellular vesicular motion.

Filipin Inhibits Endocytic Internalization of Sterols from the Plasma Membrane

After filipin treatment, particles with strong fluorescence appeared in the cortical cytoplasm of the tips of growing root hairs. To address the question of their origin, we applied the styryl dye FM4-64. In control root hairs, rapid endocytosis of FM4-64 was detected mainly in the tip, where it caused a bright fluorescence signal within the clear zone. The internalized dye labeled highly dynamic vesicles and putative early endosomes. Putative early endosomes moved both in the apical and subapical region of the root hair (Figures 4A and 4B). Slowly moving large endosome-like compartments (the putative late endosomes) up to 60 min and finally the tonoplast within 2 h of treatment were labeled later on (Ovečka et al., 2005).

Growing root hairs (Figure 4A) were pretreated with 10 $\mu g \cdot mL^{-1}$ filipin, which induced sterol labeling and complexation (Figures 4C and 4E), and were then labeled with FM4-64. Surprisingly, FM4-64 entered the root hair very rapidly at the tip and remained there trapped in fused particles and larger aggregates closely associated with the plasma membrane in the apex and lateral subapical flanks (Figure 4D). FM4-64 labels these filipin-positive compartments in the tip so rapidly because they are still physically connected with the plasma membrane. In nongrowing root hairs (Figure 4F), only the plasma membrane was labeled by filipin (Figure $1A_3$). No detectable uptake of sterols and no FM-positive particles could be seen inside of nongrowing root hairs (Figure 4G). As fused membrane-associated particles and larger aggregates were typical of filipin-sterol complexation (Figures $1A_2$, 1G to $1I_2$, 3D, and 4E; see Supplemental Figure 4E online) and internalized FM4-64 in root hairs labels early endocytic

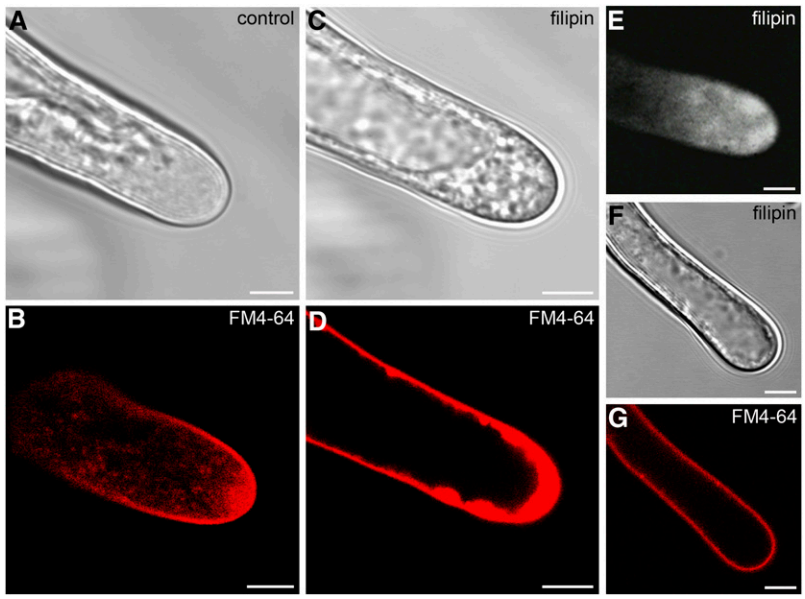

Figure 4. Pattern of Endocytosis after Complexation of Sterols.

(A) In control growing root hairs, the tip is filled with cytoplasm and fast-moving vesicles.
(B) Rapid uptake of FM4-64–labeled plasma membrane occurs in growing root hairs in control conditions. Plasma membrane, vesicles in the clear zone, and putative early endosomes in the tip and subapical region are brightly stained.
(C) The pattern of organization in the tip changes after filipin treatment. Cytoplasm is still present in the tip, but large immobilized globular particles appear.
(D) Complexation of sterols with filipin altered the pattern of endocytosis in the tip. FM4-64 was added to a root hair pretreated with filipin for 15 min (shown in **[C]**). Sterol-containing immobilized particles in the tip coaccumulated with the endocytosis marker FM4-64.
(E) Typical staining pattern after sterol complexation with filipin, when immobilized globular particles and large membrane-associated compartments are strongly filipin positive.
(F) and **(G)** In nongrowing root hairs, only the plasma membrane was labeled by FM4-64 after filipin treatment. Bright-field (**[A]**, **[C]**, and **[F]**), fluorescence **(E)**, and confocal (**[B]**, **[D]**, and **[G]**) microscopy images.
Bars = 5 μm in **(A)** to **(G)**.

compartments (Figure 4B; Ovečka et al., 2005), coaccumulation of sterol-positive (Figures 1G to $1G_2$ and 4E) and FM-positive (Figure 4D) compartments indicates that sterols within the apical compartments of root hair tips accumulate either by endocytosis or by dynamic vesicular recycling at the tip.

Simultaneous treatment of growing root hairs with filipin and FM4-64 resulted in the accumulation of both probes: the clustered, filipin-labeled particles in the tip (Figure 5A) were also FM4-64 positive (Figure 5B). Time-lapse observations of the probe uptake showed a concurrent increase of sterol- (Figure 5C) and FM-positive pools (Figure 5D) in apical compartments. The morphology and intracellular redistribution of the early endocytic/vesicular recycling compartments seemed to be primarily affected. Furthermore, the treatment revealed an inhibition of both filipin-sterol and FM4-64 uptake in the developing bulge. Filipin-positive sterols accumulated with great accuracy in the cortical cytoplasm of the bulging domain only (Figure $1E_2$). These domains also accumulated FM4-64 (Figure $1E_2$). However, filipin caused early endocytic compartments to anchor at the plasma membrane in the bulge and hindered their further redistribution, indicating that internalization by endocytosis was inhibited. The cessation of root hair tip growth at higher filipin concentration (Figure 3A) may reflect irreversible toxic effects of this drug. However, based on a continuation of reduced uptake of both probes (Figures 5C and 5D), we rather propose that filipin exerts a specific effect on sterols accumulated in the apical plasma membrane.

Complexation of Sterols Causes Structural Malformations of the Plasma Membrane

We used cryo field emission scanning electron microscopy of frozen, fully hydrated, and freeze-fractured samples for a detailed, three-dimensional examination of the cell membranes. The plasma membrane of root cells in the meristem was smooth and well stretched (Figures 6A and 6B). Only some regular longitudinal protuberances arranged in parallel to each other were recognized, and they represent imprints of the cellulose microfibrils of the cell wall inner face (Figure 6B). Application of 10 $\mu g \cdot mL^{-1}$ filipin caused no change in the structure of the tonoplast and other membranous organelles in the cytoplasm. The structure of the plasma membrane, however, was altered due to the formation of filipin-sterol complexes. We observed particles of 60 to 70 nm in diameter (in the fully hydrated state), which were regularly distributed on the cell surface. They were detected on the cell wall–plasma

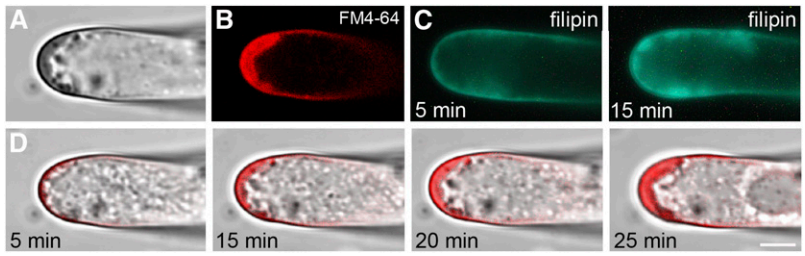

Figure 5. Endocytosis and Further Trafficking of Endocytic Compartments after Sterol Complexation.

(A) and **(B)** A root hair treated with filipin for 30 min contains large accumulated clusters in the apical part. All these clusters are FM4-64 positive; the dye was applied 10 min after filipin treatment.

(C) Filipin-positive clusters in the tip increase constantly (5 and 15 min after filipin application).

(D) Sequential treatment of a growing root hair with 10 $\mu g \cdot mL^{-1}$ filipin for 10 min followed by 4 μM FM4-64. Time-lapse observation of the uptake reveals time-dependent increase of FM4-64 content inside enlarging clusters in the tip of root hairs.

DIC **(A)**, fluorescence **(C),** confocal **(B)**, and confocal-DIC merged images **(D)**. Bar = 5 μm.

membrane interface layer. Large sheets of plasma membrane locally detached from the cell wall displayed such a pattern of damage while other membrane surfaces like the tonoplast inner leaflet remained smooth (Figure 6C). The membrane structure was interrupted by small holes of uniform size (Figure 6D). The distribution of the holes resembled the particle pattern seen in the plasma membrane adjacent to the cell wall (Figure 6C). In addition, the size of holes fitted the size of the particles (Figure 6E). Apparently, these novel particles that appeared in the plasma membrane of *Arabidopsis* root cells after filipin treatment represented filipin-sterol complexes. These results provided structural evidence that complexation of sterols by filipin caused considerable morphological damage in the plasma membrane.

Distribution and Motility of Late Endosomal Compartments after Sterol Complexation

Complexation of sterols affected the motility of vesicles and other particles in the clear zone and in the subapical domain of the cytoplasm (Figure 3D; see Supplemental Figure 4 online). Thus, for visualization of the distribution and movement of endosomes, we used transgenic *Arabidopsis* lines stably expressing green fluorescent protein (GFP)-tagged late endosomal protein reporters, such as RabF2a and double FYVE. RabF2a-positive endosomes moved actively in the apical and subapical regions of growing root hairs, although they did not frequently invade the apical dome (Figure $7A_1$; see Supplemental Movie 9 online). Immediately after complexation of sterols, the movement of RabF2a-GFP–tagged endosomes was reduced considerably and continued only in a restricted area (Figure $7A_2$; see Supplemental Movie 10 online). After filipin treatment, however, RabF2a-positive late endosomes were not found in the area where filipin-positive apical compartments had formed (Figure $7A_2$).

In control conditions, the late endosomal compartments visualized by the double FYVE-GFP construct occurred mostly in the subapical region and in the cytoplasm-containing part of the root hair (Figure 7B; see Supplemental Movie 11 online). Treatment with 10 $\mu g \cdot mL^{-1}$ of filipin induced the formation of filipin-positive apical compartments, but the general distribution of endosomal compartments as visualized with the double FYVE-GFP construct was not dramatically changed. They were mostly found in subapical and organelle-containing zones, but not in the extreme apex, where filipin-positive apical compartments were formed (Figures $7B_1$ and $7B_2$). Movement of FYVE-positive endosomes in the subapical region, however, was altered after complexation of sterols. FYVE-positive endosomes near to larger organelles such as round vacuoles showed a reduced mobility. Nevertheless, some movement of individual FYVE-positive compartments still occurred between the vacuole and the tip, as long as the compartments remained at some distance from the apical domain (Figure 7C). As they arrived at the apex and touched the clusters with complexed sterols, they became immobile (Figure 7C; see Supplemental Movie 12 online). These results indicate that complexation of sterols may affect normal membrane/vesicle exchange toward the late endosomes. However, these late endosomal compartments are not involved in the formation of filipin-positive apical complexes after filipin treatment.

Altered Motility of Late Endosomes Is Not the Primary Cause of Tip Growth Inhibition

To determine whether growth inhibition of root hairs results from the reduced motility of the late endosomal compartments caused by filipin treatment, we studied growth recovery after washing out the filipin. After treatment with different concentrations of filipin with specific dose-dependent effects, we washed root hairs with fresh medium without filipin. As both concentration and duration of the treatment are critical, we determined the intracellular motility in root hairs treated with filipin for 25 min. Using a low filipin concentration, neither tip growth (Figures 3A and 3B) nor cytoplasmic motility was altered. Recovery after treatment with 1 $\mu g \cdot mL^{-1}$ filipin followed by washing revealed a normal architecture and distribution of the FYVE-GFP compartments (Figure 8A). Also, vesicle motility in the clear zone and spreading of FYVE-positive endosomes in the apex and subapex of the root hair was normal (see Supplemental Movie 13 online). Similar observations were made after washing the root hairs pretreated with 3 $\mu g \cdot mL^{-1}$ filipin (Figure 8B). Both cytoplasmic streaming and

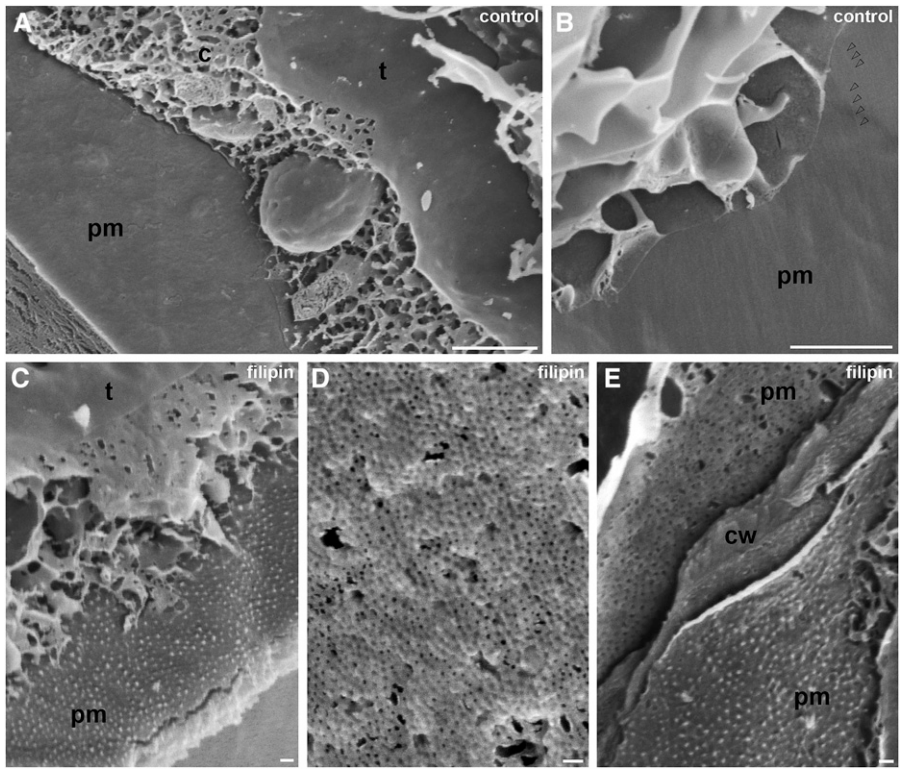

Figure 6. Integrity of the Plasma Membrane after Sterol Complexation.

(A) and **(B)** Smooth internal surface of the plasma membrane (pm) and internal surface of the tonoplast (t) in freeze-fractioned root cells. Other membranous organelles are embedded in the reticulated layer of cytosol (c) between the vacuole and the plasma membrane. Parallel protuberances in the plasma membrane caused by the cellulose microfibrils of the cell wall are indicated by arrowheads **(B)**.

(C) to **(E)** Morphology of membranes after treatment of roots with 10 $\mu g \cdot mL^{-1}$ filipin for 30 min. The structure of the tonoplast is unchanged; however, the plasma membrane adjacent to the cell wall contains dot-like structures. These particles of similar size and shape have regular distribution **(C)**. Portions of the plasma membrane detached from the cell wall display holes of similar size, shape, and pattern of distribution **(D)**. Inspection of a cell wall fragment (cw) reveals a particle-like pattern of filipin-sterol complexes in the cytosolic leaflet and a hole-like pattern in the extracellular leaflet of the plasma membrane **(E)**. This pattern indicates that filipin-sterol complexes are localized in the outer leaflet of the plasma membrane.

Bars = 1 μm in **(A)** and **(B)** and 100 nm in **(C)** to **(E)**.

motility of FYVE-positive endosomes recovered completely. However, after this treatment (3 $\mu g \cdot mL^{-1}$), the apical zone of the plasma membrane remained more brightly stained (Figure 8B; see Supplemental Movie 14 online). Although movement of FYVE-positive endosomes as well as cytoplasmic streaming in general was altered considerably in root hairs treated with 10 $\mu g \cdot mL^{-1}$ filipin (Figures $7B_1$ to 7C; see Supplemental Movies 5 and 12 online), washing out of filipin restored both cytoplasmic streaming and the fast movement of the FYVE-GFP compartments (Figure 8C; see Supplemental Movie 15 online). Apical filipin-positive compartments, which developed during the filipin treatment, persisted after washing. After direct physical contact with these compartments, FYVE-GFP–labeled endosomes were fixed there (arrows in Figure 8C). The rest of the FYVE-specific endosomes, however, remained motile (Figure 8C; see Supplemental Movie 15 online). These data indicate that although filipin reduces movement of the late endosomal compartments in a concentration-dependent manner, this is not the prime reason for the tip growth inhibition. The irreversible inhibition of root hair tip growth by high concentrations of filipin is likely to reflect some toxic effect of this inhibitor. Large artificial complexes formed at the tips of root hairs after filipin treatment may affect membrane functionality but not cell viability. This is evidenced by normal cytoplasmic streaming after washing out of filipin (Figure 8; see Supplemental Movies 13 to 15 online) and by plasmolysis of the filipin-stained root hairs (see Supplemental Figure 3 online). Dead protoplasts or protoplasts with considerable damage to the integrity of the plasma membrane would not plasmolyse.

Nature of Filipin-Induced Apical Compartments

Apparently, the tip growth of root hairs treated with higher concentrations of filipin cannot be restored due to the formation of artificial sterol-rich compartments at the tip. To reveal the underlying effect of filipin on the physiological and mechanical properties of the root hair tip, we determined the distribution of different organelle markers after filipin treatment. Cytosolic GFP occupied the entire internal volume of the apex in growing root

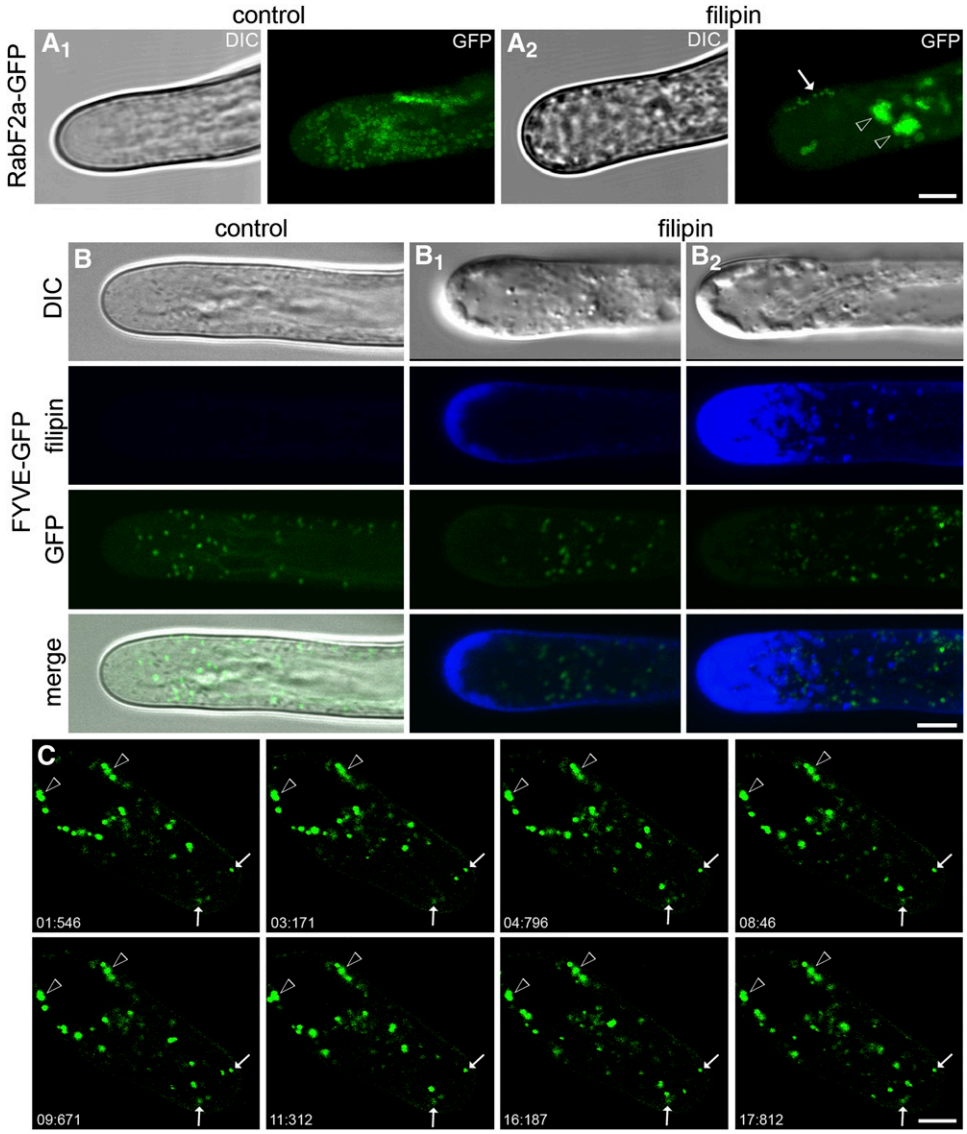

Figure 7. Motility of Late Endosomal Compartments after Filipin Treatment.

(A_1) and **(A_2)** Endosomes visualized by RabF2a-GFP. Endosomes moved actively in the apex and subapical region of growing root hairs **(A_1)**. Filipin treatment for 15 min reduced movement of RabF2a-positive endosomes to Brownian motion only (arrowheads in **[A_2]**). Only a few individual endosomes continued to move in a restricted area and over short distances (arrow in **[A_2]**). Summary maximal projections from 15 serial confocal sections in fixed Z-position without averaging.

(B) Effect of filipin on the distribution of endosomal compartments visualized by the double FYVE-GFP construct. Endosomes are distributed mostly in the subapical region and in the cytoplasm-containing part of the root hair in control conditions **(B)**. Distribution is not dramatically changed by filipin treatment (10 $\mu g \cdot mL^{-1}$ filipin for 25 min). These compartments are not involved in the formation of filipin-positive apical complexes as documented in single a median section **(B_1)** and in whole z-projections **(B_2)**.

(C) Confocal microscopy. Motility of endosomes visualized by the double FYVE-GFP construct after filipin treatment. Time-lapse imaging shows movement of FYVE-positive endosomes after complexation of sterols with filipin. Endosomes in the vicinity of the larger round vacuole reduced their movements (arrowheads). Endosomes arrived at the apical domain close to the region of clustered sterols became completely immobilized (arrows). Time is indicated in seconds.

Representative still image from Supplemental Movie 3 (DIC image in **[A_1]**), Supplemental Movie 9 **(**GFP image in **A_1),** Supplemental Movie 4 (DIC image in **[A_2]**), Supplemental Movie 10 (GFP image in **[A_2]**), Supplemental Movie 11 (GFP image in **[B]**), and sequence of images from Supplemental Movie 12 online **(C)**. Bars = 5 μm in **(A)** to **(C)**.

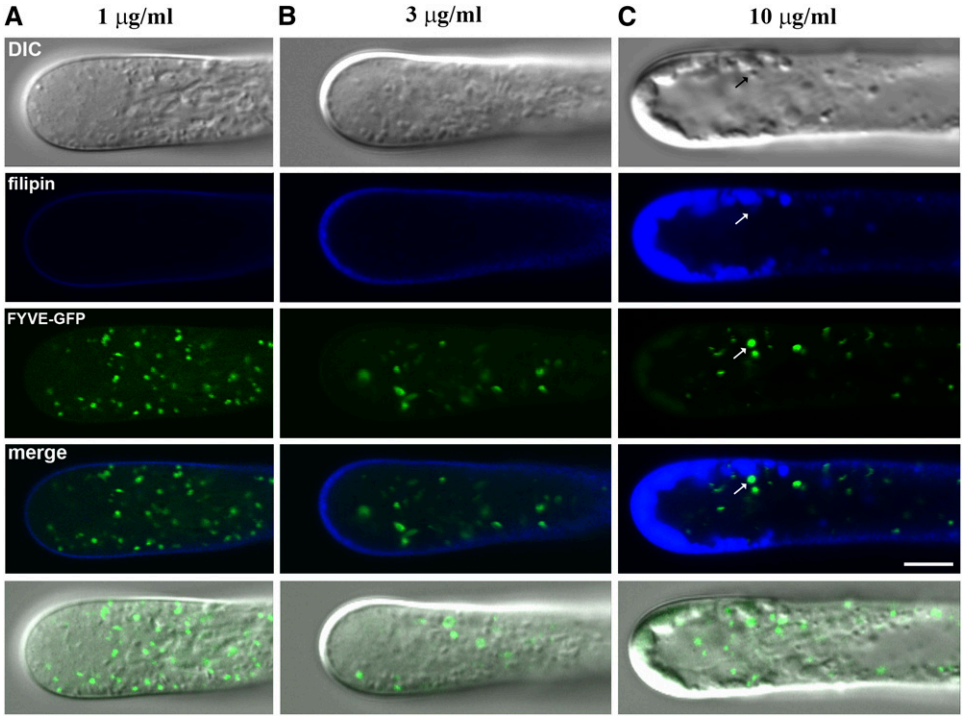

Figure 8. Motility of Endosomes Visualized by the Double FYVE-GFP Construct after Recovery from Filipin Treatment.

Root hairs treated with different concentrations of filipin for 25 min and washed out with fresh medium. Both cytoplasmic streaming and endosomal motility were completely recovered in root hairs pretreated with 1 $\mu g \cdot mL^{-1}$ filipin **(A)** and 3 $\mu g \cdot mL^{-1}$ filipin **(B)**. The motility of endosomal compartments visualized by the double FYVE-GFP construct was also recovered in root hairs pretreated with 10 $\mu g \cdot mL^{-1}$ filipin **(C)**, but FYVE compartments in close contact with filipin-positive apical compartments (arrow in **[C]**) remained immobilized after recovery. Note the stable pattern of filipin staining after washing. DIC (top row) and single confocal planes (rows 2 to 4). Row 5 in each panel: representative image of GFP-DIC merged image from Supplemental Movies 13 **(A)**, 14 **(B)**, and 15 **(C)** online. Bar = 5 μm.

hairs because of their abundance in the cytosol. Only organelles and other membranous compartments could be identified as spots that did not fluoresce in a cytoplasmic GFP background (Figure 9A). Treatment with 10 $\mu g \cdot mL^{-1}$ filipin induced the formation of filipin-positive apical compartments that were strictly separated from the cytosolic GFP (Figure 9A). This finding indicates the membranous but not cytosolic nature of filipin-positive apical compartments.

GFP fused to the HDEL-endoplasmic reticulum (ER) retention sequence was used to visualize dynamic ER profiles in growing root hairs. ER was absent from the vesicle-rich apical dome but was distributed throughout the apical and subapical zones (Figure 9B). In addition to apical filipin-positive compartments, filipin treatment (10 $\mu g \cdot mL^{-1}$) also induced the appearance of stress ER bodies in the subapical zone of root hairs. Importantly, filipin-positive apical compartments were negative for the HDEL ER retention sequence GFP marker (Figure 9B). Thus, we can conclude that the ER was not involved in the formation of filipin-positive compartments.

Mitochondria expressing the F_1-ATPase γ-subunit-GFP moved actively within the entire root hair, including the subapex, but only rarely invaded the apical clear zone (Figure 9C). Although after filipin treatment (10 $\mu g \cdot mL^{-1}$) mitochondria were found much closer to the extreme root hair apex, they were absent from the filipin-positive apical compartments (Figure 9C).

Using GFP targeted to plastid-localized ADP-sugar pyrophosphatase, we observed the expected results. The plastids were not found in the apex of growing root hairs under control conditions (Figure 9D). Root hairs treated with 10 $\mu g \cdot mL^{-1}$ filipin showed the typical effects on organelle distribution. However, plastids were not involved in the formation of the filipin-positive apical compartments (Figure 9D).

Together, these data showed no colocalization of cytosolic, ER, mitochondrial, and plastidial markers with filipin-induced apical compartments. These appear to be formed independently of cellular organelles/compartments that are largely excluded from the clear zone and not directly involved in vesicular recycling/endocytosis and regulation of root hair tip growth.

Formation of Filipin-Induced Apical Compartments Depends on Trans-Golgi Network/Early Endosomal Compartments

The large apical compartments induced by filipin treatment in the root hair tips represent a mechanical barrier that prevents the continuation of regulated tip growth. To determine which cellular

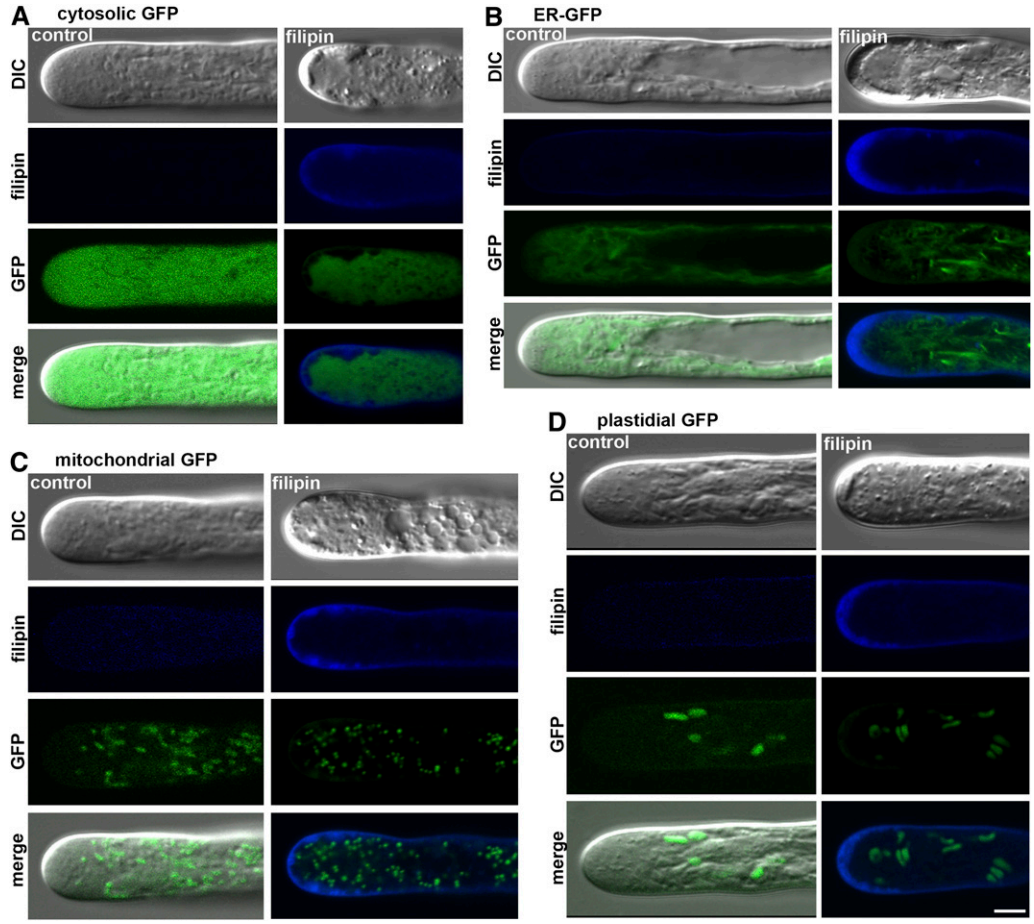

Figure 9. Distribution of the Cytosol and Organelle Markers after Filipin Treatment.

(A) Cytosolic GFP expression marks the entire volume of the cytosol in growing root hairs with the exception of membranous compartments and organelles in control conditions. Filipin-positive apical compartments formed after a 25-min treatment with 10 $\mu g \cdot mL^{-1}$ filipin are GFP negative and are separated from the cytosol.

(B) The ER-GFP construct labels dynamic ER profiles distributed throughout the root hair, with the exception of the apical dome in control conditions. A 25-min treatment with 10 $\mu g \cdot mL^{-1}$ filipin leads to the formation of apical compartments that are negative for the ER marker.

(C) The mitochondrial GFP construct labels mitochondria actively moving in the whole root hair but only rarely in the extreme apex in control conditions. A 25-min treatment with 10 $\mu g \cdot mL^{-1}$ filipin results in the movement of mitochondria into the apex but not into filipin-positive apical compartments.

(D) GFP expression in plastids shows these large organelles far from the extreme apex in control conditions. A 25-min treatment with 10 $\mu g \cdot mL^{-1}$ filipin revealed that plastids do not participate in the formation of filipin-positive apical compartments. DIC image (top row in each panel), single confocal planes (rows 2 and 3 in each panel), and confocal-DIC or filipin-GFP merged images (last row in each panel).

Bar = 5 μm.

constituents participate in the formation of these compartments, the endomembrane/vesicular compartments indispensable for tip growth should be identified. Therefore, we tested the behavior of the trans-Golgi network (TGN) marker Wave line 13 (VTI12) fused with yellow fluorescent protein (YFP) and RabA1d, a member of the RabA subfamily of small Rab GTPases, fused with GFP. The fluorescence signal of the GFP-RabA1d–expressing line was highly concentrated in the vesicle-rich apical dome of growing root hairs (Figure 10A), suggesting that RabA1d is a reliable marker for secretory/recycling vesicles in the clear zone. The pattern of the GFP-RabA1d distribution closely followed the pattern of FM4-64 staining in control root hairs, and not surprisingly, these two markers highly colocalized not only in the tip's clear zone but also in early endosomal/TGN compartments throughout the hair tube (Figure 10A). Another TGN marker, VTI12-YFP, decorated dot-like structures moving in the apical and subapical zones, and in the rest of growing root hairs, albeit with less apparent accumulation in the clear zone compared with GFP-RabA1d (Figure 11). After formation of filipin-positive apical compartments due to treatment with 10 $\mu g \cdot mL^{-1}$ of filipin, both these early endosomal/TGN molecular markers colocalized with the filipin-specific signal in the tip. Thus, both GFP-RabA1d and VTI12-YFP coaccumulated with filipin in the plasma membrane and in apical compartments closely associated with the inner

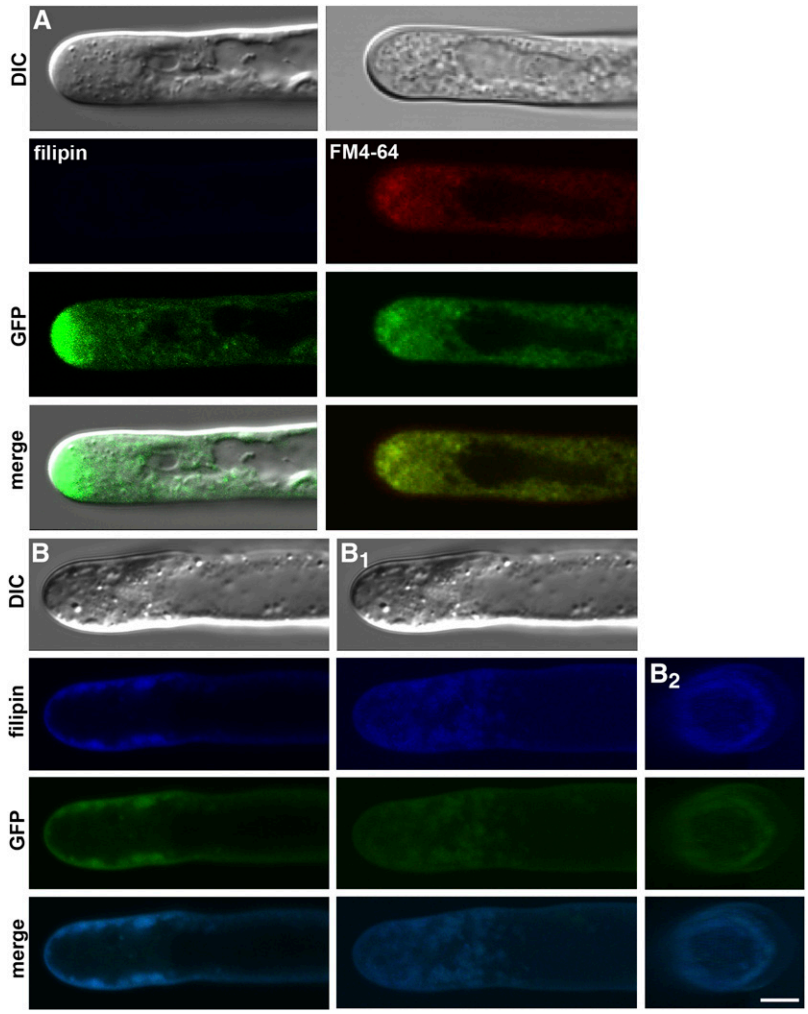

Figure 10. Effect of Filipin Treatment on the Distribution of GFP-RabA1d.

(A) GFP-RabA1d strictly accumulated in the apical dome of the growing root hair and completely colocalized with FM4-64 in control conditions. A 25-min treatment with 10 μg·mL^{-1} filipin led to the formation of filipin-positive apical compartments that colocalized with the GFP-RabA1d signal. This is documented in a single median section view **(B)**, in a whole z-projection view **(B_1)**, and in a rotated image of a transversal section of the subapical zone **(B_2)**. DIC image (top row in **[A]**, **[B]**, and **[B_1]**), single confocal planes (rows 2 and 3 in each panel), and confocal-DIC (last row in left panel in **[A]**), confocal GFP-FM4-64 (last row in right panel in **[A]**), and confocal filipin-GFP (last row in **[B]** to **[B_2]**) merged images. Bar = 5 μm.

face of the plasma membrane (Figures 10B to 10B_2 and 11). These data that demonstrate the localization of two independent TGN/early endosomal markers in growing root hairs together with their accumulation in the filipin-positive apical compartments provide a direct link between the effects of filipin and endocytic membrane trafficking and recycling at the growing tip. Moreover, these results clarify why these filipin-positive compartments are formed only at the tip of growing root hairs, where membrane trafficking activity is the highest.

DISCUSSION

Root hair growth is an example of highly polarized tip growth that is also characteristic of pollen tubes in plants. Fungal hyphae and neuronal growth cones and spines also show this mode of polarized cell growth (Guirland et al., 2004; Kamiguchi, 2006; Araujo-Bazán et al., 2008; Higuchi et al., 2009). Recently, endocytic recycling and structural sterols have emerged as pivotal players in the establishment and maintenance of polarity (de Graaf et al., 2005; Ovečka et al., 2005; Voigt et al., 2005b; Araujo-Bazán et al., 2008; Higuchi et al., 2009; Lee et al., 2009). This is a rather surprising twist in our understanding of eukaryotic cell polarity because vesicles of the TGN, which fill up the tip growing cell domain, represent both secretory vesicles and also endocytic recycling vesicles (for review, see Šamaj et al., 2006). Previous studies characterized tip-localized secretory and endosomal vesicles in root hairs (Sherrier and VandenBosch, 1994; Preuss et al., 2004, 2006; Ovečka et al., 2005; Voigt et al., 2005b),

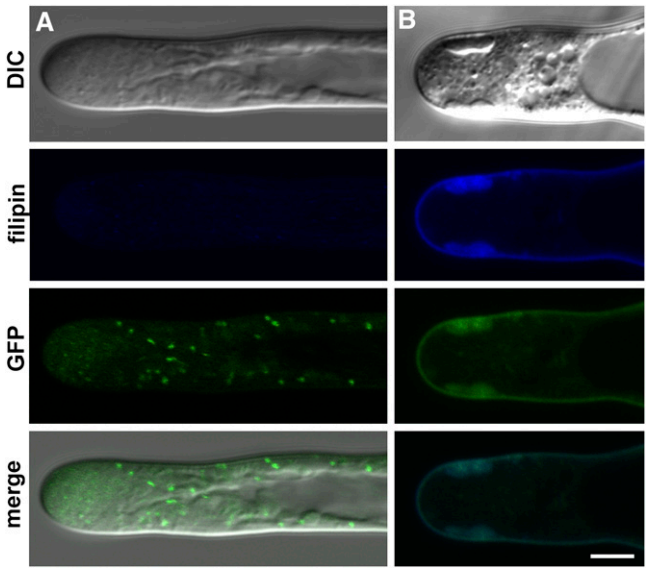

Figure 11. Effect of Filipin Treatment on the Distribution of VTI12-YFP.

(A) Distribution of dynamic compartments accumulating VTI12-YFP in a growing root hair at control conditions.

(B) Treatment with 10 $\mu g \cdot mL^{-1}$ filipin for 25 min led to the formation of filipin-positive apical compartments. The VTI12-YFP signal is restricted to the plasma membrane and to filipin-positive apical compartments. Both markers colocalized completely.

DIC image (top row in **[A]** and **[B]**), single confocal planes (rows 2 and 3 in **[A]** and **[B]**), confocal-DIC merged image (last row in **[A]**), and confocal filipin-YFP merged image (last row in **[B]**). Bar = 5 μm.

pollen tubes (Derksen et al., 1995; de Graaf et al., 2005; Wang et al., 2005; Chen et al., 2006; Bove et al., 2008; Zonia and Munnik, 2008; Lee et al., 2009; Szumlanski and Nielsen, 2009), fungal hyphae (Steinberg 2007a, 2007b; Araujo-Bazán et al., 2008; Higuchi et al., 2009), and neurons (Guirland et al., 2004; Kamiguchi, 2006). The main outcome of these studies was that vesicular recycling and endocytosis provide spatial and temporal clues for the establishment and maintenance of polarity.

A breakthrough has been achieved by defining structural sterols as leading players in the establishment of polarity cues and landmarks that subsequently attract downstream polarity determinants (for plants, see Lindsey et al., 2003). Structural sterol-rich domains, so-called detergent-resistant membrane microdomains (DRMs) or lipid rafts, were found to be upstream of all known polarity landmarks, including the exocyst components in fungal tip-growing cells (Takeshita et al., 2008). They assemble into distinct domains that recruit diverse polarity-determining molecules as well as spatially organize endocytosis and endocytic recycling in a manner that allows the generation of a highly polarized tip-growing domain (Wachtler et al., 2003; Martin and Konopka, 2004; Takeda and Chang, 2005; Wachtler and Balasubramanian, 2006; Alvarez et al., 2007; Fischer et al., 2008; Takeshita et al., 2008; Liu et al., 2009). These findings prompted us to study a possible role for structural sterol-rich domains in *Arabidopsis* root hairs. Our data reveal that filipin-labeled structural sterols represent one of the early prebulge markers at the future root hair site. Other markers include locally occurring events, such as cell wall thinning and bulging out of the weakened cell wall (Čiamporová et al., 2003; Ovečka et al., 2005), lowering of the cell wall pH (Bibikova et al., 1998), accumulation of cell wall proteins, including xyloglucan endotransglycosylase (Vissenberg et al., 2001), expansins (Baluška et al., 2000; Cho and Cosgrove, 2002), and arabinogalactan proteins (Šamaj et al., 1999), accumulation of ROP-type GTPases ROP2 and ROP6 (Molendijk et al., 2001; Jones et al., 2002; Sorek et al., 2007), and accumulation of NADPH oxidase AtrbohC/RHD2 (*Arabidopsis thaliana* respiratory burst oxidase homolog C/ROOT HAIR DEFECTIVE2; Foreman et al., 2003; Takeda et al., 2008).

To study the distribution and trafficking of sterols, we used fuorescence labeling by filipin, a polyene sterol binding probe used for the fluorescent detection of plant 3-β-hydroxy sterols. Close interactions between structural sterol-enriched domains, vesicular recycling, and endocytosis were reported for plant (Grebe et al., 2003; Boutté et al., 2009), fungal (Valdez-Taubas and Pelham, 2003; Alvarez et al., 2007; Fischer et al., 2008; Takeshita et al., 2008), and algal (Klima and Foissner, 2008) cells. In fact, sterol-enriched domains do not only serve as endocytic platforms, but they are also recycled together with endocytic vesicles (Grebe et al., 2003). Here, we show that complexation of structural sterols with filipin in the highly polar root hairs affects the distributions, motilities, and structures of TGN and other types of early endosomes, which in turn leads to rapid cessation of tip growth. Similar effects can also be deduced from root hair phenotypes of several *Arabidopsis* mutants with disrupted biosynthesis and composition of structural sterols (Jang et al., 2000; Schrick et al., 2000, 2002, 2004; Souter et al., 2002; Posé et al., 2009). Furthermore, our data suggest a novel role of structural sterols during the establishment of polarity cues in plants and in root hair tip growth. Thus, local enrichment of structural sterols reactive to filipin serves as a reliable and predictive polarity marker for the root hair outgrowth site in the prebulge stage, as well as for branching points in *Arabidopsis* mutant *tip1*, which has disturbed tip growth, and *hydra2*, which has changed homeostasis of structural sterols. This polar pattern of sterol distribution corresponds well with the developmental program of membrane polarization in other systems like *Candida albicans*, where it occurs during hyphal morphogenesis (Martin and Konopka, 2004). In *C. albicans*, before hyphal outgrowth, cells showed an intense filipin labeling at the presumptive site of germ tube formation, while during the subsequent hyphal tip growth, staining was detected at the tip. Additionally, sterol accumulation pattern correlates only with sites of active cell growth in ectopically growing tips of branched yeast cells and also in mating projections (Wachtler et al., 2003). In plants, localization of the small GTPase ROP6 to DRMs/lipid rafts has been reported recently to be essential for the polarity signaling by this signaling protein (Sorek et al., 2010). *S*-acylation of ROP6 prevented its localization to DRMs/lipid rafts and caused loss of the ROS gradient and cell polarity as well as inhibition of apical endocytosis in root hairs of *Arabidopsis* (Sorek et al., 2010).

Our data show that polarly localized structural sterol domains may function as a platform for organizing vesicular recycling and endocytosis in tip-growing root hairs. Supporting evidence for

such a role is provided by sterol accumulation in plant endomembrane systems, where these sterols preferentially colocalize with TGN/early endosomal markers (KNOLLE, ARF1, and RabA2a) in *Arabidopsis* root cells (Boutté et al., 2009). In addition, altered sterol composition in the *cpi1-1* mutant of *Arabidopsis* causes defects in clathrin-dependent endocytosis (Men et al., 2008; Boutté et al., 2009). As sterol complexation by cyclic polyene antibiotics like filipin may cause membranes to become permeable to ions and small molecules (Kinsky 1970), the resulting sequestration of sterols and serious defects in the plasma membrane should not be ignored. Inhibition of caveolae-mediated endocytosis in mammalian cells after filipin-induced caveolae disruption (Rothberg et al., 1990; Schnitzer et al., 1994) may support this scenario. Thus, the irreversible inhibition of root hair tip growth by high concentrations of filipin should be interpreted with caution and may rather reflect some toxic effects of this inhibitor, in this case affecting more processes than its function in organizing plasma membrane endocytosis. Nevertheless, concentration-dependent responses to filipin reported here, like growth rates of root hairs, motility of organelles, and complexation of particles solely in the tip of the root hairs, seem to reveal the specificity and physiological relevance of the filipin treatment in these tip-growing cells. Our data document that the formation of filipin-induced apical compartments by sequestration of sterols at the plasma membrane represent a serious mechanical and physiological barrier for tip growth continuation. This is caused by the fast and specific reaction of filipin with sterols specifically enriched in the growing root hair tip. As plasma membrane DRMs are enriched with not only structural sterols but also numerous protein kinases (Mongrand et al., 2004; Borner et al., 2005; Morel et al., 2006; Lefebvre et al., 2007; Minami et al., 2009) and likely with other signaling proteins such as small GTPases (Sorek et al., 2010), they might serve as subcellular signaling platforms. Future studies might reveal whether DRMs enriched with structural sterols maintain their putative signaling properties during vesicle trafficking and endocytic recycling.

METHODS

Plant Material and Cultivation

Seeds of *Arabidopsis thaliana* were surface sterilized and placed on Murashige and Skoog medium supplemented with vitamins, 1% sucrose, and 0.4% Phytagel (Sigma-Aldrich), and pH was adjusted to 5.8. Seeds were cold stabilized at 4°C for 48 h in Petri dishes and then grown at 22 to 24°C under continuous light. Seedlings 1 to 2 d after germination were transferred to microscope slides that were modified into thin chambers using cover slips according to Ovečka et al. (2005). Chambers were filled with the same medium without Phytagel (liquid medium) and placed in sterile glass cuvettes containing the liquid medium at a level that reached the open lower edge of the chambers. This allows the free exchange of medium between chambers and the cuvette. Seedlings were grown in vertical position under continuous light for 12 to 24 h. During this period, the seedlings stabilized root growth and proceeded to form new root hairs. The isolation of *Arabidopsis* mutants and development of transgenic lines used in this study were described previously: the *tip1* mutant with the phenotype of branching root hairs at the early stage of hair outgrowth where double, triple, or quadruple branches are formed from the bulge (Schiefelbein et al., 1993; Ryan et al., 1998), the *hydra2* mutant affecting the sterol biosynthetic pathway at the level of sterol C-14 reductase and expressing a branching root hair phenotype (Jang et al., 2000; Schrick et al., 2000; Souter et al., 2002), transgenic *Arabidopsis* lines stably expressing the GFP-tagged double FYVE construct (Voigt et al., 2005b), GFP-tagged Rab GTPase RabF2a (Voigt et al., 2005b), the GFP-tagged mitochondria-targeting presequence of the N terminus of the F_1-ATPase γ-subunit (Niwa et al., 1999), GFP containing the chimeric gene for cytosolic fusion protein pMAT-SGFP (Mano et al., 1999), GFP fused to the HDEL ER retention sequence mGFP5 (Haseloff et al., 1997), plastid-localized ADP-sugar pyrophosphatases from potato (*Solanum tuberosum*; St ASPP) fused with GFP (Muñoz et al., 2008), and the TGN marker Wave line 13 (VTI12) fused with YFP (Sanderfoot et al., 2000; Geldner et al., 2009). RabA1d (a member of the RabA subfamily of small Rab GTPases) fused with GFP (cloning and plant transformation is described below) was used as a second TGN marker in this study.

Cloning of the 35S:GFP:RabA1d Construct and Stable Plant Transformation

The coding sequence of *RabA1d* was PCR amplified from *Arabidopsis* Columbia-0 ecotype cDNA using the following primers: forward, 5′-GC**GGATCC**GTGTTAATGGCGGGTT-3′; reverse, 5′-GC**GGATCC**TTTAGGACATAAGACCAT-3′. *Bam*HI restriction sites (in bold) were used to ligate the coding sequence into the *pCAT-GFP* vector. The resulting *35S:GFP:RabA1d* expression cassette was excised by Hind*III* and ligated into the binary vector *pCB302* (Xiang et al., 1999). The construct was used to transform competent *Agrobacterium tumefaciens* GV3101 strain cells. *Arabidopsis* plants of the ecotype Columbia-0 were transformed by the *A. tumefaciens*–mediated floral dip method according to Clough and Bent (1998).

Treatments and Data Acquisition

Only seedlings with young root hairs growing at average growth rates were selected. For this aim, plants stabilized in chambers filled with control culture medium were transferred to the microscope. A selected root hair was positioned on the screen of the computer attached to the videorecorder and the microscope at time 0 and recorded for the measurement of root hair growth rate for 15 min without any mechanical perturbation. Subsequently, the chamber was gently and slowly perfused with culture medium for 10 min directly on the microscope stage. Since the volume of the chambers was ~50 μL, we used double the amount of solution (100 μL), which guaranteed a complete replacement of solutions. The speed of perfusion was 10 $\mu L \cdot min^{-1}$. The morphology and shape of the root hair apex were checked every 5 min during the perfusion. This was used also for repositioning of the root hair tip before further recording. After perfusion, the tip growth of the same root hair was measured during an additional 15 min. This ensured that no artifacts in the morphology and tip growth of root hairs were induced by the medium exchange. Only those root hairs that showed normal average speed of tip growth were used for further experiments. Therefore, the chamber was perfused with culture medium containing drugs of interest. After perfusion, tip growth of the same root hair was recorded for 15 min. Data presented were repeated in 3 to 12 independent experiments and processed using Microsoft Excel software.

Within each period of observation (15 min), root hairs were recorded every 5 min for short 5-s slots. This short recording time was chosen to prevent harmful effects of the intense microscope illumination at high magnification. Measurements of root hair elongation were made directly from the monitor screen using the play back function of the video recorder. The position of the tip was marked at the start of the 15-min period, and new positions of the tip were marked every 5 min from time-lapse images. When the hair grew out of the field of view of the camera, the hair apex was repositioned during the recording time.

Sterol Labeling and Depletion

Sterols were localized by filipin III (Sigma-Aldrich), a polyene antibiotic fluorochrome for plant 3-β-hydroxysterols (Grebe et al., 2003). Working solutions of filipin in the culture medium (0.1 to 10 $\mu g \cdot mL^{-1}$) were made from a stock solution of 25 $mg \cdot mL^{-1}$ in DMSO (final concentration of DMSO in working solution was 0.04% or lower). Most of the data presented were produced with 10 $\mu g \cdot mL^{-1}$ filipin, which provided sufficiently strong fluorescence. Chemicals were applied by the perfusion method described above.

Filipin and FM4-64 Double Labeling

The styryl dye FM 4-64 (*N*-(3-triethylammoniumpropyl)-4-(8-(4-(diethylamino)phenyl)hexatrienyl)pyridinium dibromide) (Molecular Probes) at a final concentration of 4 μM in the culture medium was infiltrated into the chambers by perfusion loading for 5 min at a speed of 10 $\mu L \cdot min^{-1}$. After 5 min, the chamber was perfused with culture medium for 5 min at the same speed and examined in the microscope. For filipin treatment, sequential loading of the chamber with 10 $\mu g \cdot mL^{-1}$ filipin for 10 or 15 min was followed by loading with 4 μM FM4-64 for 5 min. Alternatively, both dyes were applied together.

Microscopy

Video microscopy was performed as described by Lichtscheidl and Foissner (1996). Briefly, the bright-field image from a Univar microscope (Reichert-Leica), equipped with a HBO 200 mercury arc lamp, ×40 plan apo oil immersion objective (numerical aperture of 1.00), and ×1.6 additional magnification was collected by a high-resolution video camera (Chalnicon C 1000.1; Hamamatsu), processed by a digital image processor (DVS 3000; Hamamatsu), and recorded on digital video tape (JVC). Adaptation of the gain and contrast of the camera and additional improvement of the image by the image processor allowed for the visualization of small structures and vesicles in the tip of root hairs. Images and video scenes were imported into a personal computer (Sony Vaio) and measured on the screen for root hair growth and organelle motility.

Fluorescence was observed either in the same objective in the Univar or in a routine microscope (Labophot, Nikon; BX51, Olympus) with common filter sets for UV and blue light excitation. The images were documented either on a Nikon Coolpix digital photo camera or with a low-light sensitive video camera (Photonic Science) and further improved by the digital image processor (DVS 3000; Hamamatsu). Confocal microscopy of filipin-sterol complexes was performed with a FV1000 confocal microscope (Olympus) equipped with an LD 405-nm diode laser and an emission filter of 415 to 470 nm. Samples were observed using ×63 oil immersion objectives. Observations of FM4-64 and GFP-tagged chimera protein distribution were performed with a confocal laser scanning microscope Leica SP2 (ICS Leica Microsystems) equipped with ×40 and ×63 oil immersion plan apo objectives.

Scanning cryoelectron microscopy observations were performed on *Arabidopsis* plants 2 d after germination. Seedlings grown on agar plates were placed on stubs and frozen immediately by plunging into nitrogen slush. Frozen samples were transferred under vacuum using a cryotransfer unit into the ALTO cryo-preparation chamber (ALTO 2500; Gatan). Inside the cryopreparation chamber, samples were freeze fractioned, etched, sputter coated, and transferred immediately to the field emission scanning electron microscopy stage (JEOL JSM6330F version 1.04). Samples were examined at an accelerating voltage of 3 kV at −90°C.

Analysis of Organelle Motility

Organelle motility and their trajectories of movement in the tip of growing root hairs were measured from the monitor screen using the frame-by-frame playback function of the digital video tape recorder (JVC). We used video sequences that monitored the velocity of organelles in the tip of young root hairs recorded in longitudinal view or recorded from the top view (upside down direction in root hairs growing close to the cover slip). The period of recording was 10 min from which we selected 2-s time slots for the measurement. The speed of recording was 25 frames per s. Particles moving in the focal plane within ~10 frames lasting at least 0.4 s were selected. Positions of selected organelles were marked in every frame of the video sequence directly on the monitor screen using transparency overlay. In some samples, several frames were superpositioned on each other using the function of summary maximal intensity projection of a Leica SP2 confocal laser scanning microscope to display the integrated picture. Preparation of single images from the video sequences for documentation was made using a computer and Pinnacle Studio 8.8 software (Pinnacle Systems).

Accession Number

Sequence data from this article can be found in the Arabidopsis Genome Initiative or GenBank/EMBL databases under accession number At4g18800 for *RabA1d*.

Supplemental Data

The following materials are available in the online version of this article.

Supplemental Figure 1. Determination of Growing and Nongrowing Root Hairs for Sterol Localization Experiments.

Supplemental Figure 2. Distribution of Endosomal Compartments Visualized by the Double FYVE-GFP Construct in the Early Prebulge Stage.

Supplemental Figure 3. Effect of Plasmolysis on Root Hairs after Filipin Treatment.

Supplemental Figure 4. Motility of Vesicles in the Tip of Growing Root Hairs after Complexation of Sterols.

Supplemental Movie 1. 180° Rotation of a Three-Dimensional Reconstructed Trichoblast in the Prebulge Stage of Development.

Supplemental Movie 2. 180° Rotation of a Three-Dimensional Reconstructed Trichoblast in the Stage of Bulge Formation.

Supplemental Movie 3. Cytoarchitecture, Organization, and Motility of Vesicular Organelles in the Tip of a Control Root Hair.

Supplemental Movie 4. Alterations in the Distribution and Movement of Vesicles in the Tip of Growing Root Hairs after Complexation of Sterols with 10 $\mu g \cdot mL^{-1}$ Filipin for 15 min.

Supplemental Movie 5. The Presence of Filipin-Positive Apical Compartments in the Tip of a Root Hair and the Altered Movement of Particles and Cytoplasmic Streaming after a 30-Min Treatment with 10 $\mu g \cdot mL^{-1}$ Filipin.

Supplemental Movie 6. Unaffected Cytoplasmic Streaming in a Vacuolated Root Hair after a 30-Min Treatment with 10 $\mu g \cdot mL^{-1}$ Filipin.

Supplemental Movie 7. Unaffected Cytoplasmic Streaming in an Atrichoblast after a 30-Min Treatment with 10 $\mu g \cdot mL^{-1}$ Filipin.

Supplemental Movie 8. Unaffected Cytoplasmic Streaming in Cortex Cells after a 30-Min Treatment with 10 $\mu g \cdot mL^{-1}$ Filipin.

Supplemental Movie 9. Motility of RabF2a-GFP–Tagged Endosomes in a Control Root Hair.

Supplemental Movie 10. Motility of RabF2a-GFP–Tagged Endosomes after Treatment with 10 $\mu g \cdot mL^{-1}$ Filipin for 15 min.

Supplemental Movie 11. Distribution and Motility of FYVE-GFP Compartments in a Control Root Hair.

Supplemental Movie 12. Reduced Motility of Endosomes Visualized by the Double FYVE-GFP Construct after a 15-Min Treatment with 10 $\mu g \cdot mL^{-1}$ Filipin.

Supplemental Movie 13. Normal Distribution of FYVE-GFP Compartments and Their Normal Motility in the Tip of a Root Hair Treated with 1 $\mu g \cdot mL^{-1}$ Filipin for 25 Min Followed by Filipin Washout.

Supplemental Movie 14. Normal Motility of FYVE-GFP Compartments in the Tip of a Root Hair Treated with 3 $\mu g \cdot mL^{-1}$ Filipin for 25 Min Followed by Filipin Washout.

Supplemental Movie 15. Normal Distribution of FYVE-GFP and Their Normal Motility in the Tip of a Root Hair Treated with 10 $\mu g \cdot mL^{-1}$ Filipin for 25 Min Followed by Filipin Washout.

Supplemental Movie Legends.

ACKNOWLEDGMENTS

This work was supported by Grant APVV-0432-06 from the Slovak Research and Development Agency, Grant 2/0200/10 from the Scientific Grant Agency of Slovak Ministery for Education and Slovak Academy of Sciences (Bratislava, Slovakia), Grant L433-B17 from the Austrian Fonds zur Förderung der Wissenschaftlichen Forschung, Slovak Biotechnologic Center, and by structural research grants from the European Union and the Czech Republic to the Centre of the Region Haná for Biotechnological and Agricultural Research, Faculty of Science, Palacký University, Olomouc, Czech Republic (Project CZ.1.05/2.1.00/01.0007). We thank Diedrik Menzel for providing M.O. with access to the confocal laser scanning microscopy core facility at Institute of Cellular and Molecular Botany, Bonn, Daniel von Wangenheim for his help with seeds, as well as Niko Geldner, Erik Nielsen, Kathrin Schrick, and Liam Dolan for providing published material. We thank anonymous reviewers for their valuable comments and improvements.

Received July 7, 2009; revised July 21, 2010; accepted August 18, 2010; published September 14, 2010.

REFERENCES

Alvarez, F.J., Douglas, L.M., and Konopka, J.B. (2007). Sterol-rich plasma membrane domains in fungi. Eukaryot. Cell **6:** 755–763.

Andème-Onzighi, C., Sivaguru, M., Judy-March, J., Baskin, T.I., and Driouich, A. (2002). The *reb1-1* mutation of *Arabidopsis* alters the morphology of trichoblasts, the expression of arabinogalactan-proteins and the organisation of cortical microtubules. Planta **215:** 949–958.

Araujo-Bazán, L., Peñalva, M.A., and Espeso, E.A. (2008). Preferential localization of the endocytic internalization machinery to hyphal tips underlies polarization of the actin cytoskeleton in *Aspergillus nidulans.* Mol. Microbiol. **67:** 891–905.

Arnqvist, L., Dutta, P.C., Jonsson, L., and Sitbon, F. (2003). Reduction of cholesterol and glycoalkaloid levels in transgenic potato plants by overexpression of a type 1 sterol methyltransferase cDNA. Plant Physiol. **131:** 1792–1799.

Bach, T.J., and Benveniste, P. (1997). Cloning of cDNAs or genes encoding enzymes of sterol biosynthesis from plants and other eukaryotes: Heterologous expression and commentation analysis of mutations for functional characterization. Prog. Lipid Res. **36:** 197–226.

Bacia, K., Schwille, P., and Kurzchalia, T. (2005). Sterol structure determines the separation of phases and the curvature of the liquid-ordered phase in model membranes. Proc. Natl. Acad. Sci. USA **102:** 3272–3277.

Baluška, F., Baroja-Fernández, E., Pozueta-Romero, J., Hlavačka, A., Etxeberria, E., and Šamaj, J. (2006). Endocytic uptake of nutrients, cell wall molecules, and fluidized cell wall portions into heterotrophic plant cells. In Plant Endocytosis, J. Šamaj, F. Baluška, D. and Menzel, eds (Berlin: Springer-Verlag), pp. 19–35.

Baluška, F., Salaj, J., Mathur, J., Braun, M., Jasper, F., Šamaj, J., Chua, N.-H., Barlow, P.W., and Volkmann, D. (2000). Root hair formation: F-actin-dependent tip growth is initiated by local assembly of profilin-supported F-actin meshworks accumulated within expansin-enriched bulges. Dev. Biol. **227:** 618–632.

Benveniste, P. (1986). Sterol biosynthesis. Annu. Rev. Plant Physiol. **37:** 275–307.

Benveniste, P. (2005). Prenyllipids and their derivates: Sterols, prenylquinones, carotenoids and terpenoids. In Plant Lipids. Biology, Utilization and Manipulation, D.J. Murphy, ed (Oxford, UK: Blackwell Publishing), pp. 353–387.

Bessoule, J.-J., and Moreau, P. (2004). Phospholipid synthesis and dynamics in plant cells. In Lipid Metabolism and Membrane Biogenesis. Topics in Current Genetics, Vol. 6, G. Daum, ed (Berlin Heilderberg, Germany: Springer-Verlag), pp. 89–124.

Bibikova, T.N., Jacob, T., Dahse, I., and Gilroy, S. (1998). Localized changes in apoplastic and cytoplasmic pH are associated with root hair development in *Arabidopsis thaliana.* Development **125:** 2925–2934.

Bibikova, T.N., Zhigilei, A., and Gilroy, S. (1997). Root hair growth in *Arabidopsis thaliana* is directed by calcium and an endogenous polarity. Planta **203:** 495–505.

Borner, G.H.H., Sherrier, D.J., Weimar, T., Michaelson, L.V., Hawkins, N.D., MacAskill, A., Napier, J.A., Beale, M.H., Lilley, K.S., and Dupree, P. (2005). Analysis of detergent-resistant membranes in *Arabidopsis*. Evidence for plasma membrane lipid rafts. Plant Physiol. **137:** 104–116.

Boutté, Y., Frescatada-Rosa, M., Men, S., Chow, C.-M., Ebine, K., Gustavsson, A., Johansson, L., Ueda, T., Moore, I., Jürgens, G., and Grebe, M. (2009). Endocytosis restricts *Arabidopsis* KNOLLE syntaxin to the cell division plane during late cytokinesis. EMBO J. **29:** 546–558.

Bove, J., Vaillancourt, B., Kroeger, J., Hepler, P.K., Wiseman, P.W., and Geitmann, A. (2008). Magnitude and direction of vesicle dynamics in growing pollen tubes using spatiotemporal image correlation spectroscopy and fluorescence recovery after photobleaching. Plant Physiol. **147:** 1646–1658.

Campanoni, P., and Blatt, M.R. (2007). Membrane trafficking and polar growth in root hairs and pollen tubes. J. Exp. Bot. **58:** 65–74.

Chen, Y., Chen, T., Shen, S., Zheng, M., Guo, Y., Lin, J., Baluška, F., and Šamaj, J. (2006). Differential display proteomic analysis of *Picea meyeri* pollen germination and pollen-tube growth after inhibition of actin polymerization by latrunculin B. Plant J. **47:** 174–195.

Cho, H.-T., and Cosgrove, D.J. (2002). Regulation of root hair initiation and expansin gene expression in *Arabidopsis.* Plant Cell **14:** 3237–3253.

Clough, S.J., and Bent, A.F. (1998). Floral dip: A simplified method for *Agrobacterium*-mediated transformation of *Arabidopsis thaliana.* Plant J. **16:** 735–743.

Clouse, S.D. (2002). *Arabidopsis* mutants reveal multiple roles for sterols in plant development. Plant Cell **14:** 1995–2000.

Čiamporová, M., Dekánková, K., Hanáčková, Z., Peters, P., Ovečka, M., and Baluška, F. (2003). Structural aspects of bulge formation during root hair initiation. Plant Soil **255:** 1–7.

de Graaf, B.H., Cheung, A.Y., Andreyeva, T., Levasseur, K., Kieliszewski, M., and Wu, H.M. (2005). Rab11 GTPase-regulated membrane trafficking

is crucial for tip-focused pollen tube growth in tobacco. Plant Cell **17:** 2564–2579.

Derksen, J., Rutten, T., Lichtscheidl, I.K., Dewin, A.H.N., Pierson, E. S., and Rongen, G. (1995). Quantitative analysis of the distribution of organelles in tobacco pollen tubes: implications for exocytosis and endocytosis. Protoplasma **188:** 267–276.

Diener, A.C., Li, H., Zhou, W.X., Whoriskey, W.J., and Nes, W.D. (2000). *STEROL METHYL TRANSFERASE 1* controls the level of cholesterol in plants. Plant Cell **12:** 853–870.

Dolan, L., Duckett, C., Grierson, C., Linstead, P., Schneider, K., Lawson, E., Dean, C., Poethig, S., and Roberts, K. (1994). Clonal relations and patterning in the root epidermis of *Arabidopsis.* Development **120:** 2465–2474.

Fischer, R., Zekert, N., and Takeshita, N. (2008). Polarized growth in fungi-interplay between the cytoskeleton, positional markers and membrane domains. Mol. Microbiol. **68:** 813–826.

Foreman, J., Demidchik, V., Bothwell, J.H., Mylona, P., Miedema, H., Torres, M.A., Linstead, P., Costa, S., Brownlee, C., Jones, J.D., Davies, J.M., and Dolan, L. (2003). Reactive oxygen species produced by NADPH oxidase regulate plant cell growth. Nature **422:** 442–446.

Geldner, N., Dénervaud-Tendon, V., Hyman, D.L., Mayer, U., Stierhof, Y.-D., and Chory, J. (2009). Rapid, combinatorial analysis of membrane compartments in intact plants with a multicolor marker set. Plant J. **59:** 169–178.

Grebe, M., Xu, J., Möbius, W., Ueda, T., Nakano, A., Geuze, H.J., Rook, M.B., and Scheres, B. (2003). *Arabidopsis* sterol endocytosis involves actin-mediated trafficking via ARA6-positive early endosomes. Curr. Biol. **13:** 1378–1387.

Grierson, C., and Schiefelbein, J. (April 4, 2002). Root hairs. In The Arabidopsis Book. C.R. Somerville and E.M. Meyerowitz, eds (Rockville, MD: American Society of Plant Biologists), doi/10.1199/tab.0060, http://www.aspb.org/publications/arabidopsis/.

Guirland, C., Suzuki, S., Kojima, M., Lu, B., and Zheng, J.Q. (2004). Lipid rafts mediate chemotropic guidance of nerve growth cones. Neuron **42:** 51–62.

Guirland, C., and Zheng, J.Q. (2007). Membrane lipid rafts and their role in axon guidance. Adv. Exp. Med. Biol. **621:** 144–155.

Hartmann, M.-A. (2004). Sterol metabolism and functions in higher plants. In Lipid Metabolism and Membrane Biogenesis. Topics in Current Genetics, Vol. 6, G. Daum, ed (Berlin, Heilderberg, Germany: Springer-Verlag), pp. 183–211.

Haseloff, J., Siemering, K.R., Prasher, D.C., and Hodge, S. (1997). Removal of a cryptic intron and subcellular localization of green fluorescent protein are required to mark transgenic *Arabidopsis* plants brightly. Proc. Natl. Acad. Sci. USA **94:** 2122–2127.

Higuchi, Y., Shoji, J.Y., Arioka, M., and Kitamoto, K. (2009). Endocytosis is crucial for cell polarity and apical membrane recycling in the filamentous fungus *Aspergillus oryzae.* Eukaryot. Cell **8:** 37–46.

Hobbs, D.H., Hume, J.H., Rolph, C.E., and Cooke, D.T. (1996). Changes in lipid composition during floral development of *Brassica campestris.* Phytochemistry **42:** 335–339.

Howles, P.A., Birch, R.J., Collings, D.A., Gebbie, L.K., Hurley, U.A., Hocart, C.H., Arioli, T., and Williamson, R.E. (2006). A mutation in an *Arabidopsis* ribose 5-phosphate isomerase reduces cellulose synthesis and is rescued by exogenous uridine. Plant J. **48:** 606–618.

Ibáñez, C.F. (2004). Lipid rafts as organizing platforms for cell chemotaxis and axon guidance. Neuron **42:** 3–5.

Jang, J.C., Fujioka, S., Tasaka, M., Seto, H., Takatsuto, S., Ishii, A., Aida, M., Yoshida, S., and Sheen, J. (2000). A critical role of sterols in embryonic patterning and meristem programming revealed by the *fackel* mutants of *Arabidopsis thaliana.* Genes Dev. **14:** 1485–1497.

Jones, M.A., Shen, J.-J., Fu, Y., Li, H., Yang, Z., and Grierson, C.S. (2002). The *Arabidopsis* Rop2 GTPase is a positive regulator of both root hair initiation and tip growth. Plant Cell **14:** 763–776.

Kamiguchi, H. (2006). The region-specific activities of lipid rafts during axon growth and guidance. J. Neurochem. **98:** 330–335.

Kato, M., and Wickner, M. (2001). Ergosterol is required for the Sec18/ATP-dependent priming step of homotypic vacuole fusion. EMBO J. **20:** 4035–4040.

Kinsky, S.C. (1970). Antibiotic interaction with model membranes. Annu. Rev. Pharmacol. **10:** 119–142.

Klima, A., and Foissner, I. (2008). FM dyes label sterol-rich plasma membrane domains and are internalized independently of the cytoskeleton in characean internodal cells. Plant Cell Physiol. **49:** 1508–1521.

Le, J., Vandenbussche, F., Van Der Straeten, D., and Verbelen, J.P. (2001). In the early response of *Arabidopsis* roots to ethylene, cell elongation is up- and down-regulated and uncoupled from differentiation. Plant Physiol. **125:** 519–522.

Lee, C.B., Kim, S., and McClure, B. (2009). A pollen protein, NaPCCP, that binds pistil arabinogalactan proteins also binds phosphatidylinositol 3-phosphate and associates with the pollen tube endomembrane system. Plant Physiol. **149:** 791–802.

Lee, Y., Bak, G., Choi, Y., Chuang, W.I., Cho, H.T., and Lee, Y. (2008). Roles of phosphatidylinositol 3-kinase in root hair growth. Plant Physiol. **147:** 624–635.

Lefebvre, B., Furt, F., Hartmann, M.A., Michaelson, L.V., Carde, J.P., Sargueil-Boiron, F., Rossignol, M., Napier, J.A., Cullimore, J., Bessoule, J.J., and Mongrand, S. (2007). Characterization of lipid rafts from *Medicago truncatula* root plasma membranes: A proteomic study reveals the presence of a raft-associated redox system. Plant Physiol. **144:** 402–418.

Lichtscheidl, I.K., and Foissner, I. (1996). Video microscopy of dynamic plant cell organelles: Principles of the technique and practical application. J. Microsc. **181:** 117–128.

Lindsey, K., Pullen, M.L., and Topping, J.F. (2003). Importance of plant sterols in pattern formation and hormone signalling. Trends Plant Sci. **8:** 521–525.

Liu, P., Zhang, L., Li, R., Wang, Q., Niehaus, K., Baluška, F., Šamaj, J., and Lin, J. (2009). Lipid microdomain polarization is required for NADPH oxidase-dependent ROS signaling in *Picea meyeri* pollen tube tip growth. Plant J. **60:** 303–313.

Mano, S., Hayashi, M., and Nishimura, M. (1999). Light regulates alternative splicing of hydroxypyruvate reductase in pumpkin. Plant J. **17:** 309–320.

Marsan, M.P., Bellet-Amalric, E., Muller, I., Zaccai, G., and Milon, A. (1998). Plant sterols: A neutron diffraction study of sitosterol and stigmasterol in soybean phophatidylcholine membranes. Biophys. Chem. **75:** 45–55.

Marsan, M.P., Muller, I., and Milon, A. (1996). Ability of clionasterol and poriferasterol (24-epimers of sitosterol and stigmasterol) to regulate membrane lipid dynamics. Chem. Phys. Lipids **84:** 117–121.

Martin, S.W., and Konopka, J.B. (2004). Lipid raft polarization contributes to hyphal growth in *Candida albicans.* Eukaryot. Cell **3:** 675–684.

Men, S., Boutté, Y., Ikeda, Y., Li, X., Palme, K., Stierhof, Y.D., Hartmann, M.A., Moritz, T., and Grebe, M. (2008). Sterol-dependent endocytosis mediates post-cytokinetic acquisition of PIN2 auxin efflux carrier polarity. Nat. Cell Biol. **10:** 237–244.

Menon, A.K. (2002). Lipid transport - An overview. Semin. Cell Dev. Biol. **13:** 159–162.

Minami, A., Fujiwara, M., Furuto, A., Fukao, Y., Yamashita, T., Kamo, M., Kawamura, Y., and Uemura, M. (2009). Alterations in detergent-resistant plasma membrane microdomains in *Arabidopsis thaliana* during cold acclimation. Plant Cell Physiol. **50:** 341–359.

Moeller, C.H., and Mudd, J.B. (1982). Localization of filipin-sterol

complexes in the membranes of *Beta vulgaris* roots and *Spinacia oleracea* chloroplasts. Plant Physiol. **70:** 1554–1561.

Molendijk, A.J., Bischoff, F., Rajendrakumar, C.S., Friml, J., Braun, M., Gilroy, S., and Palme, K. (2001). *Arabidopsis thaliana* Rop GTPases are localized to tips of root hairs and control polar growth. EMBO J. **20:** 2779–2788.

Mongrand, S., Morel, J., Laroche, J., Claverol, S., Carde, J.P., Hartmann, M.A., Bonneu, M., Simon-Plas, F., Lessire, R., and Bessoule, J.J. (2004). Lipid rafts in higher plant cells: purification and characterization of Triton X-100-insoluble microdomains from tobacco plasma membrane. J. Biol. Chem. **79:** 36277–36286.

Morel, J., Claverol, S., Mongrand, S., Furt, F., Fromentin, J., Bessoule, J.J., Blein, J.P., and Simon-Plas, F. (2006). Proteomics of plant detergent-resistant membranes. Mol. Cell. Proteomics **5:** 1396–1411.

Mukherjee, S., and Maxfield, F.R. (2000). Role of membrane organization and membrane domains in endocytic lipid trafficking. Traffic **1:** 203–211.

Muñoz, F.J., Baroja-Fernández, E., Ovečka, M., Li, J., Mitsui, T., Sesma, M.T., Montero, M., Bahaji, A., Ezquer, I., and Pozueta-Romero, J. (2008). Plastidial localization of a potato "Nudix" hydrolase of ADPglucose linked to starch biosynthesis. Plant Cell Physiol. **49:** 1734–1746.

Nichols, B.J., Kenworthy, A.K., Polishchuk, R.S., Lodge, R., Roberts, T.H., Hirschberg, K., Phair, R.D., and Lippincott-Schwartz, J. (2001). Rapid cycling of lipid raft markers between the cell surface and Golgi complex. J. Cell Biol. **153:** 529–542.

Niwa, Y., Hirano, T., Yoshimoto, K., Shimizu, M., and Kobayashi, H. (1999). Non-invasive quantitative detection and applications of non-toxic, S65T-type green fluorescent protein in living cells. Plant J. **18:** 455–463.

Ovečka, M., Lang, I., Baluška, F., Ismail, A., Illeš, P., and Lichtscheidl, I.K. (2005). Endocytosis and vesicle trafficking during tip growth of root hairs. Protoplasma **226:** 39–54.

Ovečka, M., and Lichtscheidl, I.K. (2006). Sterol endocytosis and trafficking in plant cells. In Plant Endocytosis, J. Šamaj, F. Baluška, and D. Menzel, eds (Berlin, Heilderberg, Germany: Springer-Verlag), pp. 117–137.

Peskan, T., Westermann, M., and Oelmuller, R. (2000). Identification of low-density Triton X-100-insoluble plasma membrane microdomains in higher plants. Eur. J. Biochem. **267:** 6989–6995.

Posé, D., Castanedo, I., Borsani, O., Nieto, B., Rosado, A., Taconnat, L., Ferrer, A., Dolan, L., Valpuesta, V., and Botella, M.A. (2009). Identification of the *Arabidopsis* dry2/sqe1-5 mutant reveals a central role for sterols in drought tolerance and regulation of reactive oxygen species. Plant J. **59:** 63–76.

Preuss, M.L., Serna, J., Falbel, T.G., Bednarek, S.Y., and Nielsen, E. (2004). The *Arabidopsis* Rab GTPase RabA4b localizes to the tips of growing root hair cells. Plant Cell **16:** 1589–1603.

Preuss, M.L., Schmitz, A.J., Thole, J.M., Bonner, H.K., Otegui, M.S., and Nielsen, E. (2006). A role for the RabA4b effector protein PI-4Kbeta1 in polarized expansion of root hair cells in *Arabidopsis thaliana.* J. Cell Biol. **172:** 991–998.

Proszynski, T.J., Klemm, R., Bagnat, M., Gaus, K., and Simons, K. (2006). Plasma membrane polarization during mating in yeast cells. J. Cell Biol. **173:** 861–866.

Rothberg, K.G., Ying, Y.S., Kamen, B.A., and Anderson, R.G. (1990). Cholesterol controls the clustering of the glycophospholipid-anchored membrane receptor for 5-methyltetrahydrofolate. J. Cell Biol. **111:** 2931–2938.

Ryan, E., Grierson, C.S., Cavell, A., Steer, M., and Dolan, L. (1998). TIP1 is required for both tip growth and non-tip growth in *Arabidopsis.* New Phytol. **138:** 49–58.

Šamaj, J., Braun, M., Baluška, F., Ensikat, H.J., Tsumuraya, Y., and Volkmann, D. (1999). Specific localization of arabinogalactan-protein epitopes at the surface of maize root hairs. Plant Cell Physiol. **40:** 874–883.

Šamaj, J., Müller, J., Beck, M., Böhm, N., and Menzel, D. (2006). Vesicular trafficking, cytoskeleton and signalling in root hairs and pollen tubes. Trends Plant Sci. **11:** 594–600.

Šamaj, J., Ovečka, M., Hlavačka, A., Lecourieux, F., Meskiene, I., Lichtscheidl, I.K., Lenart, P., Salaj, J., Volkmann, D., Bögre, L., Baluška, F., and Hirt, H. (2002). Involvement of the mitogen-activated protein kinase SIMK in regulation of root hair tip growth. EMBO J. **21:** 3296–3306.

Šamaj, J., Read, N.D., Volkmann, D., Menzel, D., and Baluška, F. (2005). The endocytic network in plants. Trends Cell Biol. **15:** 425–433.

Sanderfoot, A.A., Assaad, F.F., and Raikhel, N.V. (2000). The Arabidopsis genome. An abundance of soluble *N*-ethylmaleimide-sensitive factor adaptor protein receptors. Plant Physiol. **124:** 1558–1569.

Sherrier, D.J., and VandenBosch, K.A. (1994). Secretion of cell wall polysaccharides in *Vicia* root hairs. Plant J. **5:** 185–195.

Shigematsu, S., Watson, R.T., Khan, A.H., and Pessin, J.E. (2003). The adipocyte plasma membrane caveolin functional/structural organization is necessary for the efficient endocytosis of GLUT4. J. Biol. Chem. **278:** 10683–10690.

Scheaffer, A., Bronner, R., Benveniste, P., and Schaller, H. (2001). The ratio of campesterol to sitosterol that modulates growth in *Arabidopsis* is controlled by STEROL METHYLTRANSFERASE 2;1. Plant J. **25:** 605–615.

Schiefelbein, J., Galway, M., Masucci, J., and Ford, S. (1993). Pollen tube and root-hair tip growth is disrupted in a mutant of *Arabidopsis thaliana.* Plant Physiol. **103:** 979–985.

Schnitzer, J.E., Oh, P., Pinney, E., and Allard, J. (1994). Filipin-sensitive caveolae-mediated transport in endothelium: Reduced transcytosis, scavenger endocytosis, and capillary permeability of select macromolecules. J. Cell Biol. **127:** 1217–1232.

Schrick, K., Fujioka, S., Takatsuto, S., Stierhof, Y.D., Stransky, H., Yoshida, S., and Jürgens, G. (2004). A link between sterol biosynthesis, the cell wall, and cellulose in *Arabidopsis.* Plant J. **38:** 227–243.

Schrick, K., Mayer, U., Horrichs, A., Kuhnt, C., Bellini, C., Dangl, J., Schmidt, J., and Jürgens, G. (2000). FACKEL is a sterol C-14 reductase required for organized cell division and expansion in *Arabidopsis* embryogenesis. Genes Dev. **14:** 1471–1484.

Schrick, K., Mayer, U., Martin, G., Bellini, C., Kuhnt, C., Schmidt, J., and Jürgens, G. (2002). Interactions between sterol biosynthesis genes in embryonic development of *Arabidopsis.* Plant J. **31:** 61–73.

Simons, K., and Toomre, D. (2000). Lipid rafts and signal transduction. Nat. Rev. Mol. Cell Biol. **1:** 31–39.

Singh, S.K., Fischer, U., Singh, M., Grebe, M., and Marchant, A. (2008). Insight into the early steps of root hair formation revealed by the *procuste1* cellulose synthase mutant of *Arabidopsis thaliana.* BMC Plant Biol. **8:** 57.

Sitbon, F., and Jonsson, L. (2001). Sterol composition and growth of transgenic tobacco plants expressing type-1 and type-2 sterol methyltranferses. Planta **212:** 568–572.

Sorek, N., Poraty, L., Sternberg, H., Bar, E., Lewinsohn, E., and Yalovsky, S. (2007). Activation status-coupled transient S acylation determines membrane partitioning of a plant Rho-related GTPase. Mol. Cell. Biol. **27:** 2144–2154.

Sorek, N., Segev, O., Gutman, O., Bar, E., Richter, S., Poraty, L., Hirsch, J.A., Henis, Y.I., Lewinsohn, E., Jürgens, G., and Yalovsky, S. (2010). An S-acylation switch of conserved G domain cysteines is required for polarity signaling by ROP GTPases. Curr. Biol. **20:** 914–920.

Souter, M., Topping, J., Pullen, M., Friml, J., Palme, K., Hackett, R.,

Grierson, D., and Lindsey, K. (2002). *hydra* mutants of *Arabidopsis* are defective in sterol profiles and auxin and ethylene signaling. Plant Cell **14:** 1017–1031.

Steinberg, G. (2007a). On the move: Endosomes in fungal growth and pathogenicity. Nat. Rev. Microbiol. **5:** 309–316.

Steinberg, G. (2007b). Hyphal growth: A tale of motors, lipids, and the Spitzenkörper. Eukaryot. Cell **6:** 351–360.

Szumlanski, A.L., and Nielsen, E. (2009). The Rab GTPase RabA4d regulates pollen tube tip growth in *Arabidopsis thaliana.* Plant Cell **21:** 526–544.

Takeda, S., Gapper, C., Kaya, H., Bell, E., Kuchitsu, K., and Dolan, L. (2008). Local positive feedback regulation determines cell shape in root hair cells. Science **319:** 1241–1244.

Takeda, T., and Chang, F. (2005). Role of fission yeast myosin I in organization of sterol-rich membrane domains. Curr. Biol. **15:** 1331–1336.

Takeshita, N., Higashitsuji, Y., Konzack, S., and Fischer, R. (2008). Apical sterol-rich membranes are essential for localizing cell end markers that determine growth directionality in the filamentous fungus *Aspergillus nidulans.* Mol. Biol. Cell **19:** 339–351.

Takos, A.M., Dry, I.B., and Soole, K.L. (1997). Detection of glycosylphosphatidylinositol-anchored proteins on the surface of the *Nicotiana tabacum* protoplasts. FEBS Lett. **405:** 1–4.

Valdez-Taubas, J., and Pelham, H.R. (2003). Slow diffusion of proteins in the yeast plasma membrane allows polarity to be maintained by endocytic cycling. Curr. Biol. **13:** 1636–1640.

Vissenberg, K., Fry, S.C., and Verbelen, J.P. (2001). Root hair initiation is coupled to a highly localized increase of xyloglucan endotransglycosylase action in *Arabidopsis* roots. Plant Physiol. **127:** 1125–1135.

Voigt, B., Timmers, T., Šamaj, J., Müller, J., Baluška, F., and Menzel, D. (2005a). GFP-FABD2 fusion construct allows *in vivo* visualization of the dynamic actin cytoskeleton in all cells of *Arabidopsis* seedlings. Eur. J. Cell Biol. **84:** 595–608.

Voigt, B., et al. (2005b). Actin-based motility of endosomes is linked to polar tip-growth of root hairs. Eur. J. Cell Biol. **84:** 609–621.

Wachtler, V., and Balasubramanian, M.K. (2006). Yeast lipid rafts? An emerging view. Trends Cell Biol. **16:** 1–4.

Wachtler, V., Rajagopalan, S., and Balasubramanian, M.K. (2003). Sterol-rich plasma membrane domains in the fission yeast *Schizosaccharomyces pombe.* J. Cell Sci. **116:** 867–874.

Wang, Q., Kong, L., Li, Y., Šamaj, J., Baluška, F., and Lin, J. (2005). Effects of brefeldin A on pollen germination and tube growth: antagonistic effects on endocytosis and secretion. Plant Physiol. **139:** 1692–1705.

Willemsen, V., Friml, J., Grebe, M., van den Toorn, A., Palme, K., and Scheres, B. (2003). Cell polarity and PIN protein positioning in *Arabidopsis* require *STEROL METHYLTRANSFERASE1* function. Plant Cell **15:** 612–625.

Xiang, C., Han, P., Lutziger, I., Wang, K., and Oliver, D.J. (1999). A mini binary vector series for plant transformation. Plant Mol. Biol. **40:** 711–717.

Zonia, L., and Munnik, T. (2008). Vesicle trafficking dynamics and visualization of zones of exocytosis and endocytosis in tobacco pollen tubes. J. Exp. Bot. **59:** 861–873.